

## Image based velocity profile estimation for Pulsed Ultrasound Velocimetry

Master's thesis in Physics and Astronomy

Marlene Bonmann

**Image based velocity profile estimation  
for Pulsed Ultrasound Velocimetry**  
MARLENE BONMANN

© MARLENE BONMANN, 2014.

Department of Fundamental Physics  
Chalmers University of Technology  
SE-412 96 Gothenburg  
Sweden  
Telephone +46 (0)31-772 1000

The work has been made at:

Structure and Material Design  
SIK – the Swedish Institute for Food and Biotechnology  
SP- Technical Research Institute of Sweden  
SE-402 29 Gothenburg  
Sweden  
Telephone +46 (0)10-516 66 00

Supervisors:

Dr. Johan Wiklund, Flow-Viz/SIK – The Swedish Institute for Food and Biotechnology  
Dr. Reinhardt Kotze, Flow-Viz/Cape Peninsula University of Technology

Examiner:

Professor Fredrik Kahl  
Department of Signals and Systems  
Chalmers University of Technology

Cover

Doppler spectrum of oil as a result of Pulsed Ultrasound Velocimetry.  
The image based velocity profile estimator developed in this work was applied to determine the velocity profile shown as dotted line.





**Image based velocity profile estimation  
for Pulsed Ultrasound Velocimetry  
MARLENE BONMANN**

Department of Fundamental Physics  
Chalmers University of Technology

## ABSTRACT

A well-established, non-invasive, in-line technique for monitoring the rheological properties of a fluid in a pipe in real time is Pulsed Ultrasound Velocimetry (PUV) in combination with pressure difference measurement (PD). PUV makes it possible to determine the velocity profile along the measuring axis using Doppler echography.

One problem that is left to solve is to develop an automatic determination of the position of the pipe wall and to estimate the correct velocity close to the liquid-wall interface. Due to temperature changes, different fluids in pipe, and pipe material it is not possible to set the wall position to a fixed value.

The profile is distorted close to the wall, because the received signal is a convolution of sampling volumes with the velocity distribution of particles within the pipe. That is especially a problem when the sampling volume overlaps with both, the wall and the fluid.

It has been shown that the physical characterization of the pulse and deconvolution of the signal improve the velocity estimation. However, this method is complex and an easier and especially faster method has to be found.

In this work an image based velocity profile estimator is developed and tested for its industrial applicability.

The code for the velocity profile estimator was written in MATLAB. The image is generated from the Doppler spectrum and is then processed with the help of functions of MATLAB's Image Processing Toolbox. It was shown that the determination of the wall position with the newly developed velocity profile estimator works reliable according to the image. The user does not have to select the wall position manually anymore.

Furthermore, the shape of the velocity profile that was estimated from the automatic detected wall looks reasonable and is smoother than velocity profiles obtained with the current FFT-method, especially, when a small number of pulse repetitions was used. A really important improvement was the enhancement of the detected velocity gradient at the pipe wall. It is now realistic and thus the correct velocity can be obtained

The correct rheological properties of ketchup could be found in half of the time with the image based velocity profile estimator compared to the FFT-method because the number of pulse repetitions could be decreased.

Keywords: Doppler, Pulsed Ultrasound Velocimetry, Velocity Profile, Spectra, Image Processing



# Acknowledgement

I wish to thank Dr. Johan Wiklund and Dr. Reinhardt Kotzé for their support and advice. Thanks to their experimental work I was supplied with data and could conduct my work.

I also want to thank the whole Structure and Material Design Group that very warmly welcomed me. It was a pleasure to be part of the group.

Thank you Lotta for welcoming me every morning with a smile and a hearty “God morgon, god morgon!”

I want to thank Dr. Fredrik Kahl for being the examiner of this work.

Thank you to my friends and fellow students that accompanied me during my studies and helped me to survive the hardest times.

Last but not least I thank my parent who made it possible for me to study. I am very grateful for that.



# Nomenclature

Symbol / Abbreviation	Description Unit
C	Sound velocity [m/s]
Center Gate	Gate coordinate of the center of the pipe
d	Distance from transducer to gate [m]
D	Pipe diameter [m]
$f_d$	Frequency shift [Hz]
$f_0$	Basic ultrasound frequency [Hz]
CS	Correct Steps (function)
FFT	Fast Fourier Transform
$\dot{\gamma}$	Shear rate [1/s]
HVE	Higher Velocity Edge
I/Q data	Demodulated echo amplitude data (I = In Phase ; Q = Co Phase)
K	Prefactor of power-law
LVE	Lower Velocity Edge
$\mu$	Viscosity [Pa s]
n	Global exponential factor
$p_a$	Applied pressure [Pa]
PD	Pressure difference [Pa]
PIOV	Prevent increase of velocity (function)
$P_{max}$	Maximal measurable depth [m]
PRF	Pulse repetition frequency [Hz]
PUV	Pulsed Ultrasound Velocimetry
$\rho$	Density of fluid [kg/m <sup>3</sup> ]
R	Pipe radius [m]
Re	Reynolds number
$\tau$	Shear stress [Pa]
$\Theta$	Doppler angle
t	time [s]
US	Ultrasound
UVP	Ultrasound velocity profiling (measuring technique)
V	mean velocity of fluid in pipe [m/s]
v	velocity [m/s]
$V_{max}$	Maximal measurable velocity
W	Gate width
z	Acoustic impedance [(N s)/m <sup>3</sup> ]



# Contents

<b>Acknowledgement</b> .....	<b>iii</b>
<b>Nomenclature</b> .....	<b>v</b>
<b>1 Introduction</b> .....	<b>1</b>
<b>2 Objectives</b> .....	<b>5</b>
<b>3 Delineation</b> .....	<b>7</b>
<b>4 Background</b> .....	<b>9</b>
4.1 Rheology and Velocity Profiles.....	9
4.2 Basics of ultrasound .....	12
<b>4.2.1 Properties of pulsed ultrasound</b> .....	<b>13</b>
4.3 Pulsed Ultrasound Velocimetry .....	15
<b>4.3.1 Working principles</b> .....	<b>15</b>
<b>4.3.2 Important equations and limitations of parameter settings</b> .....	<b>17</b>
<b>4.3.3 Distortion of the spectra</b> .....	<b>18</b>
<b>4.3.4 Measurements with Flow-Viz<sup>TM</sup></b> .....	<b>24</b>
<b>5 Image based velocity profile estimation</b> .....	<b>27</b>
5.1 Signal processing .....	27
5.2 Wall detection .....	35
5.3 Profile detection .....	39
<b>5.3.1 Use both edges (BE)</b> .....	<b>41</b>
<b>5.3.2 Prevent increase of velocity (PIOV)</b> .....	<b>42</b>
<b>5.3.3 Correct steps in the profile shape (CS)</b> .....	<b>44</b>
<b>6 Evaluation of image based velocity estimator</b> .....	<b>46</b>
6.1 Test on simulation.....	46
<b>6.1.1 Description of simulation</b> .....	<b>46</b>
<b>6.1.2 Results from test on simulation</b> .....	<b>49</b>
6.2 Test of code on real measurement data .....	52
<b>6.2.1 Variation of threshold ratio</b> .....	<b>52</b>
<b>6.2.2 Variation of number of number of pulse repetitions and profile blocks</b>	<b>55</b>
<b>6.2.3 Validation of profile detection functions</b> .....	<b>60</b>

6.2.4	Rheology of ketchup .....	67
7	Conclusion and outlook .....	71
7.1	Conclusion .....	71
7.2	Outlook & Recommendations.....	72
	Bibliography.....	75

# 1 Introduction

In fluid engineering industry products ranging from chocolate, oil, paints etc. need to be transported in pipes between various processing steps in the production line. It is essential for the manufacturers to continuously monitor the process and to optimize it in order to ensure good and sustained product quality and to save energy and costs. It is most favorable that the monitoring happens in-line and in real time, because ...

The rheology ("the study of the deformation and flow of matter", (Barnes, 1993)) of the product bares important information about its flow behavior, consistency and its structure.

That information can be used to control the properties and quality of the product. Detailed knowledge about the flow properties can also help to optimize the production process and to design new novel products.

There are many different techniques available to measure rheological properties of the products (Steffe, 1996). Measurements can be done off-line or in-line, invasive or non-invasive. Off-line techniques are for example rotational rheometers or industry viscometers that require a sample removal from the production line followed by time consuming analysis in the lab. An in-line alternative are pipe viscometers with the disadvantage that they can only determine one point on the flow curve at a particular flow rate, this means that in order to obtain a complete flow curve many flow rates are needed and therefore this technique is very time consuming.

It is preferable to do the measurements in-line and non-invasive. Furthermore it might not be possible to take probes of the fluid invasively because of too high/low temperature, pressure in the pipe or the contact to the fluid has to be avoided because of the risk of contamination of the product or the fluid itself poses a health risk (e.g. paint).

An additional requirement is that the technique should work for opaque materials because 95 % of industrial fluids are opaque. Techniques based on optics, like laser Doppler velocimetry (Durst, 1976), are not suitable for opaque fluids.

The demand for an in-line and non-invasive technique makes pulsed ultrasound velocimetry (PUV) very interesting. Its working principle is based on pulsed Doppler echography. A PUV system can be applied in-line and it is a non-invasive technique. Under certain circumstances it is even possible to determine the velocity profile over the whole pipe diameter. That depends on the attenuation of the ultrasound beam by the fluid, the energy of the ultrasound and the pulse repetition frequency (PRF) (The physical properties and relations of ultrasound are explained in Section 4.2). Moreover, PUV gives instantaneous results and works even for opaque fluids. An additional pressure difference (PD) measurement enables the determination of the rheological properties (Wiklund J. a., 2007), (Wiklund J. a., 2014).

---

PUV can be described very basically as follows (a more explicit description follows in Section 4.3. A transducer emits and receives ultrasound (US) pulses. The pulses are a few cycles<sup>1</sup> (typically 2-5 cycles) long. The US pulses are reflected and scattered by particles in the fluid that have different acoustic impedance than the surrounding medium. The phase shift of two consecutive received pulses that is due to the movement of the particles is used for velocity estimation. The beam axis can be divided into gates. The depth of the gates is determined by the time between emission and reception of one pulse. The pulse has a spatial extension and the area it overlaps with is called sampling volume. Frequency domain and time domain algorithms (Barber, 1985) can be used for the signal processing and estimation of local Doppler velocities. From the velocity profile the shear rate is estimated with the gradient method (Mueller, 1997). The rheology is determined in combination with pressure drop. The volumetric flow rate is calculated by numerical integration of the measured velocity profile.

Doppler Ultrasound has especially been an important tool in medical applications for the non-invasive measurement of blood flow, (Evans, 2000). Takeda (Takeda, 1986) has developed and tested Ultrasound Velocity Profiling (UVP) for application on general fluids. Since then PUV has been extensively investigated and further developed by different groups of scientist (ISUD, 2014).

SIK and CPUT developed a complete fluids characterization system, called Flow-Viz<sup>TM</sup> which incorporates a sensor unit, a control panel and software for signal processing (Flow-Viz, 2014)<sup>2</sup>

One of the problems with PUV was the poor transducer technology with simple pencil type immersion transducers. These transducers had to be in contact with the liquid, which is not acceptable in an industrial set-up. Moreover, the conventional transducers have massive problems with attenuation (loss of energy) of the ultrasound by scattering and absorption. The attenuation affects the signal-to-noise ratio and the penetration depth. Flow-Viz<sup>TM</sup> incorporates a new type of non-invasive transducers that can transmit high energy and enable measurements through industrial stainless steel pipes.

There is direct access to the echo data, which gives the liberty to apply custom filters and algorithms that enhance the accuracy of velocity profile measurements.

The Flow-Viz<sup>TM</sup> instrument also offers much higher spatial resolution compared to commercially available instruments and choice of various velocity estimation algorithms. It is an advantage to have access to several different estimators as their performance differ from application to application., For example, time-domain algorithms work better for a low signal to noise ratio than frequency based algorithms (Kotzé R. a., 2013).

Though the technique is very far developed and tested it is still difficult to determine the accurate velocity profile shape at the wall (Kotzé R. a., 2010) and the actual liquid-wall interface. This is because the wall position changes due to temperature changes, different fluids in pipe, and pipe.

---

<sup>1</sup> The number of cycles is equivalent to the number of periods of the pulse and determines its length.

<sup>2</sup> [www.flow-viz.com](http://www.flow-viz.com)

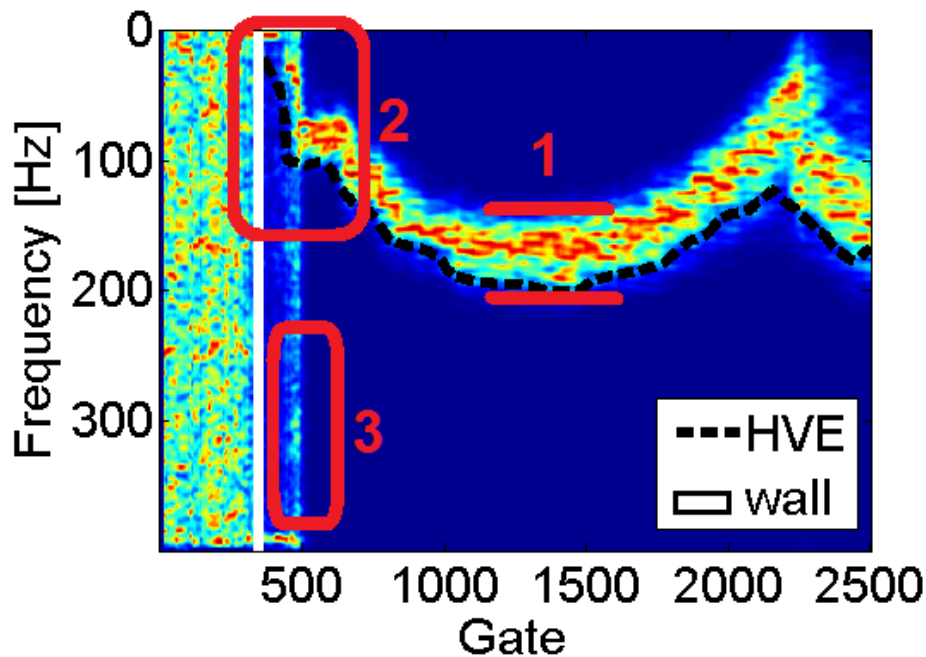


*Figure 1* Example Doppler spectrum of Oil. The higher velocity edge (HVE) and the wall position are marked. Implications that affect the profile's shape are 1: Spectral broadening. 2: Flattened profile at the wall caused by convolution. 3: Reverberation

Currently, the wall position is calculated. That is possible because the velocity of sound is known of the coupling materials and the pipe material. The coupling material allows the non-invasive measurement by guiding the ultrasound pulse inside the pipe. In order to calculate the wall position variables that are dependent onto the properties of the ultrasound pulse (length, amplification) have to be set. However, this is not accurate enough since sample volume shapes and lengths changes with changing parameter settings and different transducers, Furthermore, changes in temperature change the properties of the materials and possibly the velocity of sound in the medium. It is also possible that the pipe vibrates and then the preset wall position can be placed at the wrong distance from the transducer. It is not an ideal solution for continuous monitoring of industrial processes.

If the flow profile is parabolic it is possible to estimate the wall position by subtracting the pipe radius from the position where the velocity of the profile is maximal. This technique cannot be applied if the velocity profile is flat (plug-flow profiles, see Section 4.1, *Figure 4*). *Figure 1* shows an example of a Doppler spectrum from a measurement with oil.

---

The three main implications that affect the flow profile's shape are

1. Spectral broadening
2. Convolution of finite sample volume with true flow profile
3. Reverberation. Multiple reflection of the pulse at wall-fluid interface

Due to the distortion of the profile at the wall it is very difficult to determine the correct wall position and an appropriate velocity profile at the same time.

An accurate wall detection and shape of the velocity profile is important to be able to determine accurate flow properties Kotzé (Kotzé R. a., 2013) tested a deconvolution algorithm that improves the velocity profile's shape at the wall. For the application of this method the pulse's shape needs to be measured continuously by using two sensors which makes this approach complex and time intensive.

The aim is to be able to monitor the process in real-time while determining an accurate velocity distribution therefore time consuming procedures and algorithms are no option. High speed velocity estimation can be possible if the number of US pulses is reduced as well as the number of profile blocks<sup>3</sup> that are used for averaging. However, with less available data and averaging, conventional velocity estimators that require good signal-to-noise ratios are less accurate. Because of these reasons a new image based velocity estimator is developed and tested.

By visual inspection of the image of the Doppler spectrum (*Figure 1*) the wall position can be pointed out immediately. The higher velocity edge (HVE, edge of the profile that corresponds to higher velocities) of the flow image seems to have an appropriate shape but the wrong magnitude. It was shown by Tortoli (Tortoli, 1996) that it is possible to calculate the correct velocity profile for water from the maximal frequencies in the Doppler spectrum. The maximal frequencies correspond to the higher velocity edge.

The idea for this work was is to use image processing tools from MATLAB in order to find the wall position. From that point the correct shape of the velocity profile shall be extracted and then rescaled to the true maximum velocity value.

Since it is difficult to develop an image based velocity estimator that is applicable for all possible image qualities and shapes of the velocity profile, different optional profile detection functions were developed that can be chosen to be applied manually.

The image based velocity estimator was tested on a simple simulation and on real measurements. The simulation illustrates a moving particle suspended in liquid flow in a pipe. The real measurement data originated from measurements of Newtonian (Oil) and complex non-Newtonian fluids (ketchup and grout).

---

<sup>3</sup> The pulses received by the transducer are acquired in profile blocks with the dimension (number of gates )x (number of pulse repetitions)

## **2 Objectives**

The objective of this work was to develop an image based velocity profile estimator.

The image based velocity profile estimator should fulfill the following requirements:

- Be independent from the shape of the measuring volume, shape of the transducers, the velocity of sound and temperature
- Reliably detect the wall that is visible in the image of the Doppler spectrum.
- From the detected wall position the correct velocity profile shall be estimated.
- The processing time shall be reduced by reducing the number of pulse repetitions and overall averaging.

The image based velocity profile estimator was tested on measurement data from oil, ketchup and grout.



## **3 Delineation**

The code of the imaged based velocity profile estimator is written in MATLAB.

The data sets that were used for this work originate from measurements with the Flow-Viz<sup>TM</sup> instrument only.

The fluids that were investigated are oil, ketchup and grout because of their different flow behavior. Oil is a Newtonian fluid while ketchup is Herschel-Bulkley fluid with wall-slip and grout is a Bingham fluid.

A simulation of the Doppler signal was used to validate the velocity profile estimator. The code was originally developed by Hans Torp, Norwegian University of Science and Technology 21.Sept.02 but was modified in order to simulate one point particle in solution moving across the pipe width.



## 4 Background

### 4.1 Rheology and Velocity Profiles

Rheology is the study of the deformation and flow of matter (Barnes, 1993). The task is to find relationship between deformation and stresses.

The flow behavior of a fluid is shown in flow curves (*Figure 2*) that show the relation between shear stress  $\tau$  (force applied coplanar to the fluid's cross section) and shear rate  $\dot{\gamma}$  (rate of change in velocity  $dv$  per depth increment  $dy$ ).

The proportionality factor is the viscosity  $\mu$ . Viscosity is a measure for how well a fluid flows when a shear stress is applied. The viscosity is determined by the fluid's consistency, constituents, concentration and temperature (Rao, 2014). There are different kinds of rheometers to determine the rheology of a fluid (Steffe, 1996).

When the fluid flows through a pipe the fluid's velocity profile across the pipe diameter is dependent on the fluid's rheological properties like the viscosity and yield strain. The yield strain is the amount of shear stress that has to be exceeded before a fluid start to flow.

Likewise, that implies that it is possible to derive the rheological properties from the velocity profile's shape. One way to determine the viscosity is to fit the profile by a mathematical model that describes flow behavior, e.g. the Herschel-Bulkley model (Holdsworth, 1993).

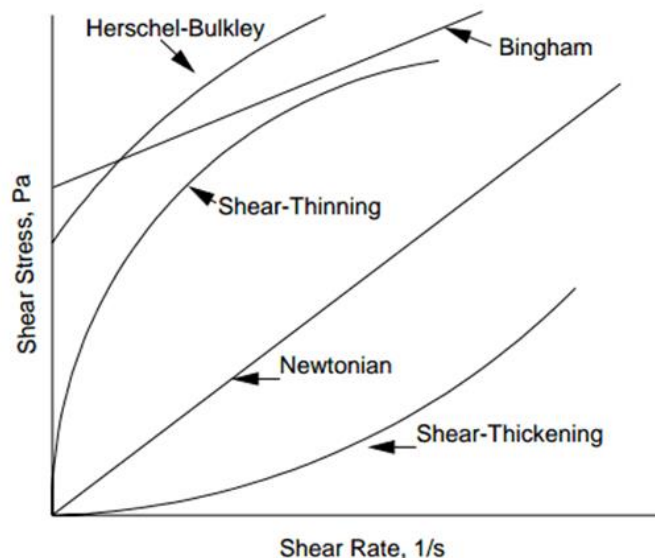


*Figure 2* Flow curves (Steffe, 1996).

---

Another approach that is not dependent on theoretical models is illustrated in Figure 3. The velocity profile is measured and the gradient method (Wiklund J. a., 2012) is applied to determine the shear rate across the pipe diameter. In order to determine the shear rate it is actually sufficient to measure the velocity profile across half the pipe diameter, because it is symmetrical along the center of the pipe.

In pipes the driving force of flow is the pressure gradient along the pipe which is generated by pumps. An additional measure of the pressure gradient  $\Delta P$  along the length  $L$  of the pipe enables the determination of the wall shear stress (Wilkinson, 1960)

$$\tau_w = \frac{R\Delta P}{2L} \quad (1)$$

where  $R$  is the pipe radius and the radial dependent shear stress

$$\tau(r) = \tau_w \frac{r}{R}. \quad (2)$$

Thus the viscosity can be determined by

$$\mu = \tau/\dot{\gamma} \quad (3)$$

Velocity profiles of fluids that do not start to flow before a certain yield stress is exceeded exhibit plug flow. The radius of the plug can be used to estimate the yield stress (Fredrickson, 1964)

*Figure 4* shows velocity profiles that result from fluids with different flow behavior. Water and oil (Ronningsen, 2012) are Newtonian fluids. Newtonian fluids have a linear relation between shear stress and shear rate. All other fluids that have a non-linear relation between shear stress and shear rate are called non-Newtonian fluids.

Most products (95%) in industry are non-Newtonian.

Ketchup is an example for a non-Newtonian fluid. Before ketchup starts to flow a certain yield stress needs to be exceeded. As soon as ketchup starts to flow it behaves like a shear thinning fluid. That means that with increasing shear stress the viscosity will decrease (gradient of curve). Ketchup can be described by the Herschel-Bulkley model. If a yield stress has to be exceeded and after that the fluid behaves like a Newtonian fluid it is called Bingham fluid, e.g. concrete (Banfill, 2003). The velocity profiles of ketchup and grout exhibit plug flow.

A shear-thickening fluid has the opposite behavior. Increasing shear stress leads to increasing viscosity.

The third velocity profile in *Figure 4* illustrates a fluid that exhibits wall-slip. If the particles in the medium consist of long chains (e.g. polymers (Hatzikiriakos, 2012)) they are aligned to the flow direction and slip along the wall if the shear stress exceeds a critical value. Hence, the velocity at the wall is not zero.

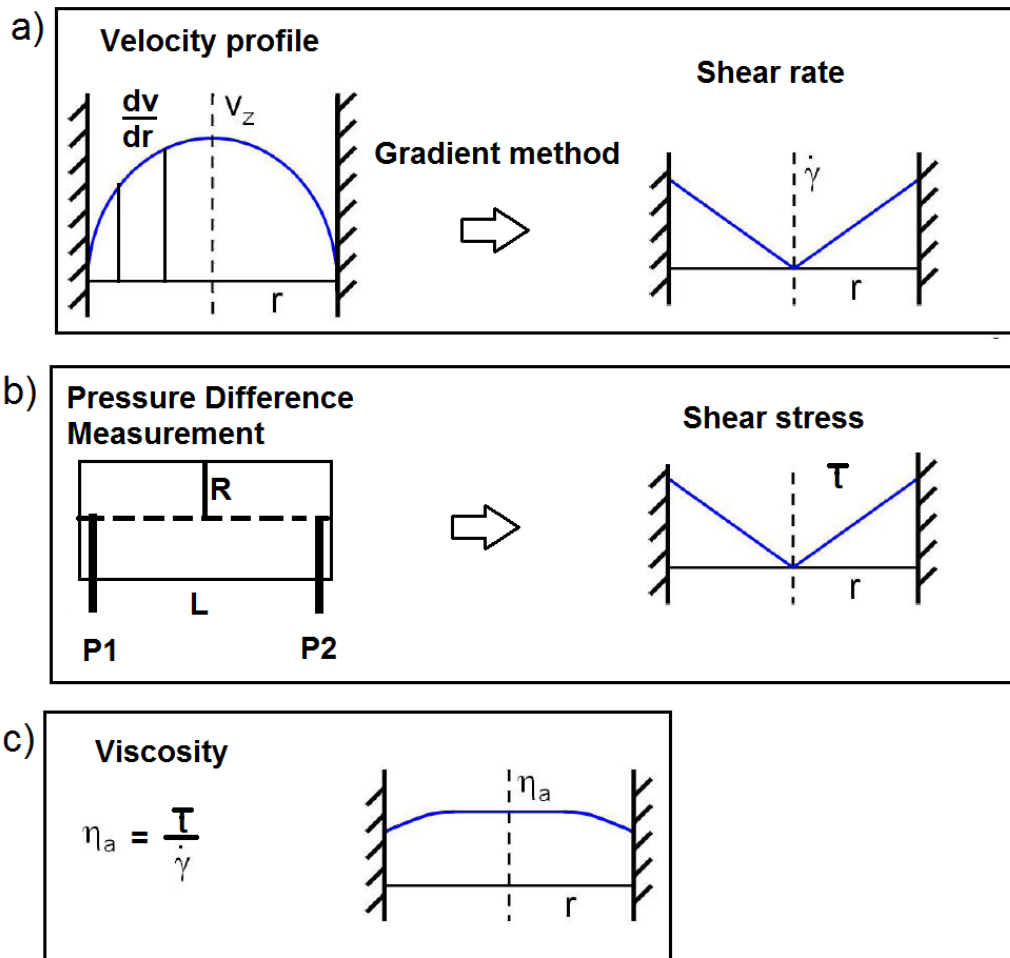


**Figure 3** Method for viscosity estimation. A) The velocity profile is measured and the gradient method applied to estimate the shear stress across the pipe diameter. B) A pressure difference measurement along the length  $L$  of the pipe is conducted and the wall shear stress  $\tau_w$  is determined. That allows the estimation of the shear stress  $\tau$ . C) The relation of shear stress to shear rate allows the estimation of the viscosity.

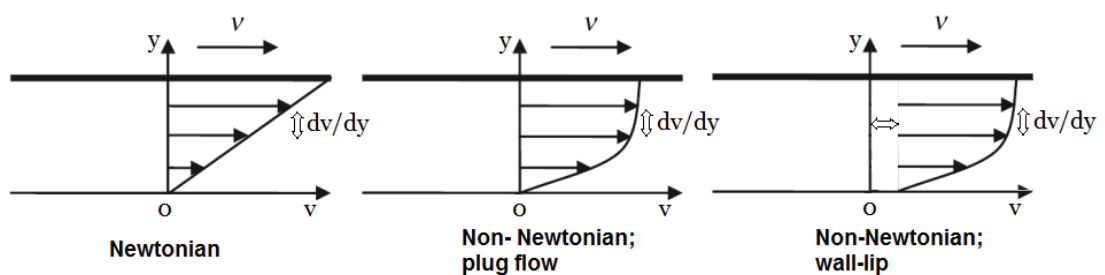


**Figure 4** Example velocity profiles. ( $dv/dy$ : shear rate.) From left to right: Water - Newtonian fluid; Ketchup - non-Newtonian fluid; Wall-slip-fluid, (modified (Klafter, 2011))

---

For the examples of velocity profiles in *Figure 4* laminar flow is assumed. Laminar, transitional and turbulent flow are distinguished with the help of the dimensionless Reynolds number. For Newtonian fluids the Reynolds number is defined as

$$Re = \frac{\rho * V * D}{\mu} \quad (4)$$

$\rho$ : Density of the fluid,  $V$ : mean velocity of the fluid in the pipe,  $D$ : internal pipe diameter,  $\mu$ : constant viscosity. Hence the fluid's velocity, density, viscosity and the pipe size determine the flow behavior.

Estimating the Reynolds number for non-Newtonian fluids is more complex because the viscosity  $\mu$  depends on the shear rate ( $\mu(\dot{\gamma})$ ). Scientists developed different generalized Reynold numbers for different flow behavior of non-Newtonian fluids (Madlener, 2009). Most fluids can be described by a power-law model and the generalized Reynolds number that is valid in that case and was introduced by Metzner and Reed is:

$$Re_G = \frac{D^n V^{2-n} \rho}{8^{n-1} K} \left( \frac{4^n}{1+3n} \right)^n \quad (5)$$

Where  $K$ : prefactor of power-law,  $n$ : global exponential factor.

For most processes in the food industry the Reynolds number is low and laminar flow is present due to high viscosity of products, e.g. chocolate.

## 4.2 Basics of ultrasound

The existence of ultrasound has first been discovered by Lazzaro Spallanzani (1729–1799). He studied how bats were able to orientate in the darkness and locate objects (Eisenberg, 1992). Since then the ultrasound technique has been developed and has a broad range of applications e.g. sonar (Hackmann, 1984), ultrasonic welding, ultrasonic cleaning (Ensminger, 2009), Doppler ultrasound (Evans, 2000). Doppler ultrasound is especially well established in medicine because it is non-invasive and a relatively inexpensive and compact technique compared to computer tomography and magnetic resonance tomography that require big and expensive instruments.

There are a vast amount of books and publications that describe the physics of ultrasound in detail e.g. Shutilov, 1988. For this work only pulsed ultrasound was used for the measurements (Pulsed Ultrasound Velocimetry explained in Section 3.3.). The application of pulsed ultrasound makes it possible to measure the velocity distribution over the pipe's cross section whereas the application of a continuous beam allows only the measurement of the average velocity in the pipe (Jones, 1993). This section summarizes the most important aspects of pulsed ultrasound.

## 4.2.1 Properties of pulsed ultrasound

Sound is the propagation of compressional longitudinal waves in a medium. Ultrasound (US) is the name for sound waves with frequencies above 20 kHz, which cannot be heard by humans. Ultrasound can be generated and received with the help of transducer. The crucial element of the transducer is a piezoelectric element that can be used to either set the adjacent medium in vibration or to receive vibrations and transform it into a voltage signal.

The shape of the ultrasound pulse is determined by the shape of the piezoelectric element and the applied voltage signal. One can imagine the transducer's active element to be split up into very little parts and every single one is a source of an ultrasound beam. The beams are overlapping and interfering and sum up to the final pulse.

It has to be distinguished between near-field and far-field of the pulse. In the near-field the pulse has unstable fluctuations of energy. It should be avoided to use the near-field for measurements. Eventually, the amplitude stabilizes and from that point the far-field begins. The pulse has its maximal intensity at the focal point.

The pulse's shape is partly responsible for the broadening of the flow profile in *Figure 1* (The causes are explained in Section 4.3.3 ).

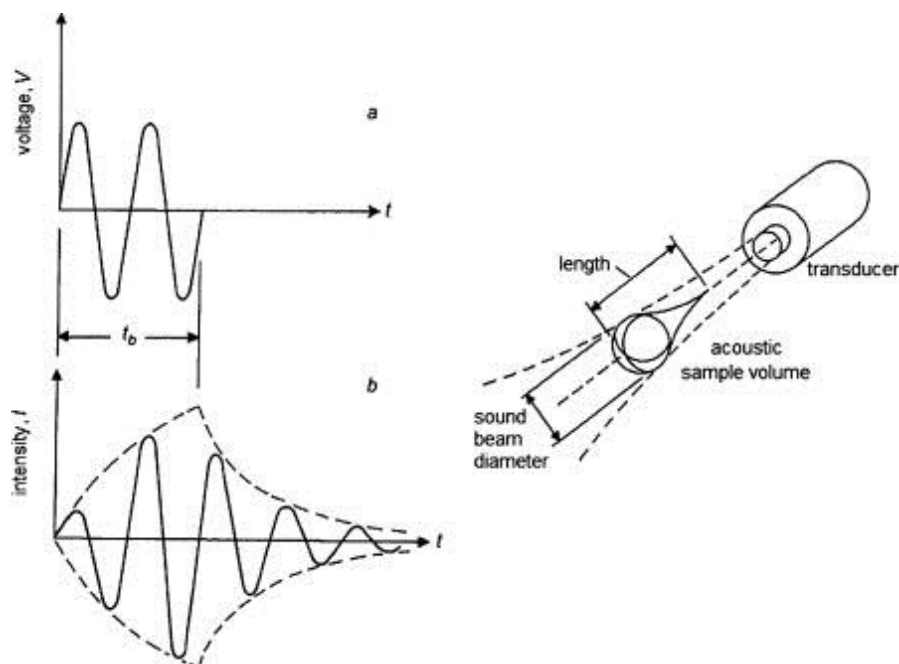


**Figure 5** Example of transducer response and sample volume geometry. A) Applied voltage signal. B) Generated pulse is drop-like shaped. (Jorgensen, 1973).

---

When the pulse is generated, its amplitude is first low then it increases to a maximum and decreases again. The pulse is shaped drop like (*Figure 5*). The velocity of the pulse in the fluid is given by

$$c \cong \left( \frac{paV}{\rho_0} \right)^{\frac{1}{2}} \quad (6)$$

Where  $\rho$ : Density of medium,  $pa$ : applied pressure.  $\frac{\Delta V}{V}$ : Fractional change in volume.

That means that the less compressible a fluid the higher the sound velocity.

Travelling through the medium the ultrasound pulse suffers reflection, refraction, scattering and absorption.

All these processes lead to the loss of energy which is summarized in the term attenuation. The degree of attenuation is dependent on the basic frequency, the medium and the temperature.

If ultrasound hits an interface of two media with different acoustic impedance  $z$

$$z = \rho_0 * c \quad (7)$$

Where  $\rho_0$ : density;  $c$ : sound velocity in medium, it is partly reflected and refracted according to Snell's Law:

$$\text{Sin}\theta_i / \text{Sin}\theta_t = c_1 * c_2 \quad (8)$$

$\theta_i$  : angle of incident;  $\theta_t$ : angle of refraction.

The sample volume geometry and the interaction of the ultrasound pulse with matter leads to distortion of the Doppler spectra.

The causes for distortion are explained in more detail in Section 4.3.3.

## 4.3 Pulsed Ultrasound Velocimetry

Pulsed ultrasound Velocimetry (PUV) is a methodology for measuring the velocity profile of a fluid across the pipes cross section. However, it is sufficient to determine the velocity profile across half pipe cross section. In this section the working principles and important equations and parameter settings and limitations of PUV are described. Furthermore, the causes for distortion of the spectra are discussed.

### 4.3.1 Working principles

Pulsed Ultrasound Velocimetry (PUV) makes it possible to determine velocity profiles in contrast to continuous Doppler ultrasound echography. If a continuous ultrasound beam is used it is only possible to estimate the average velocity over the measuring range but not the complete velocity profile.

The working principle of PUV is illustrated in *Figure 6* and *Figure 7*. The transducer is mounted to the pipe with an angle between the beam axis and flow direction. This angle is called the Doppler angle. The name originates from the Doppler Effect. The Doppler Effect is change in frequency of a sound wave if two objects are moving relative to each other. One of the objects acts as source of the wave the other one as receiver. If the source approaches the receiver the frequency is observed as higher than the emitted frequency. After the source has passed and recedes, the receiver observes the frequency as down shifted. A common example of the Doppler Effect is the change of the sound of the siren of an ambulance or police car when it is passing by.

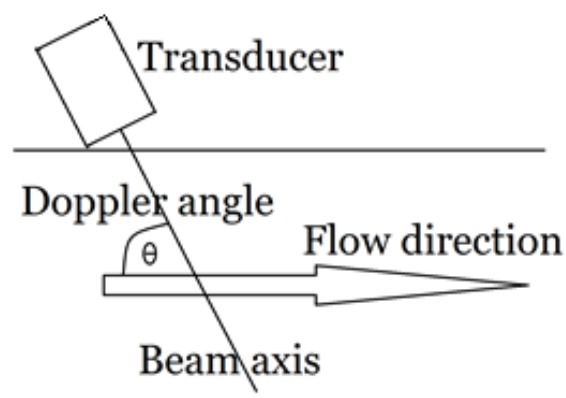


*Figure 6* Scheme Experimental Set-up and Doppler angle

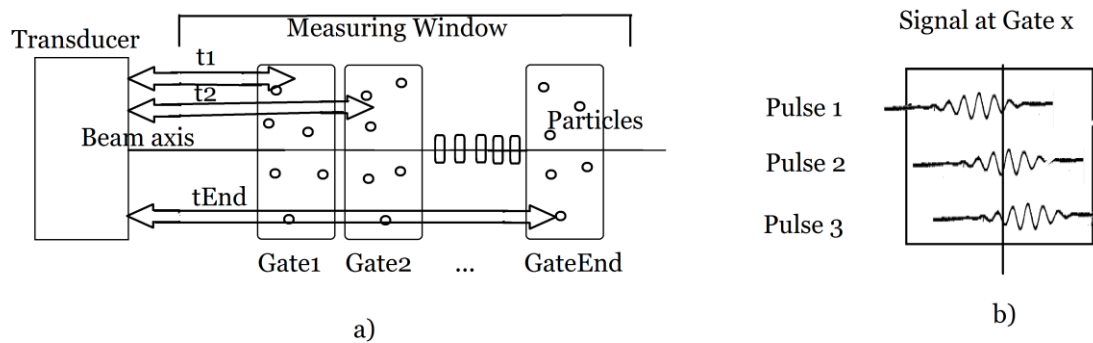


**Figure 7.** a) Principle of gates. Depth of gates is determined by the time it takes for the pulse to travel forth and back. b) Phase shift of signal, because particles move between consecutive pulses.

The velocity estimation of continuous Doppler ultrasound echography (CDUE) is based on the Doppler Effect. The Doppler angle is necessary because the particles need to move away or towards the transducer in order to be able to estimate the particle velocity.

In contrast to (CDUE), the velocity estimation principle of PUV is determined by the phase shift of consecutive received pulses ( *Figure 7 b*)). The phase shift is due to the particles' movement between the pulses. The Doppler shift cannot be detected directly for pulsed ultrasound because the Doppler shift would be in the same order as the down shift in frequency by attenuation (Jensen, 1996). However, from the phase shift between consecutive pulses it is possible to determine the Doppler frequency that is associated with the velocity by Equation 15 given in Section 4.3.2 .

In this case the Doppler angle is important to decrease the overlap of the sampling volume with the flow profile gradient in the pipe.

Successive pulses are emitted by the transducer at the pulse repetition frequency (PRF). The beam axis is separated into gates (see *Figure 7*) and the placement and size of the gate can be set by the user.

The time it takes for the pulse to travel to the gate and back to the transducer is converted into physical distance using Equation 9.

$$d = (t * c)/2 \quad (9)$$

Where  $d$ : gate distance from transducer;  $t$ : time between emitted and received pulse;  $c$ : sound velocity.

The measuring range is called the measuring window (see *Figure 7 a*)).

The pulse's interaction with matter and the pulse's shape and spatial extension as well as the width of the gate lead to distortion by refraction, attenuation, convolution, broadening of the flow profile as could be seen in *Figure 1*.

Distortion of the spectrum makes it difficult for the velocity estimation algorithms to estimate the velocity correctly. The causes of the distortion are explained in Section 4.3.3.

## 4.3.2 Important equations and limitations of parameter settings

The equations in this section are adapted from the book by Jensen (Jensen, 1996). It is important to note that the measuring parameters like the pulse repetition frequency (PRF) and the gate distance and width cannot be chosen deliberately. There are several important dependencies that have to be considered.

First of all the PRF is restricted by the time it takes for the US pulse to travel through the measuring window and back to the transducer. The relation can also be seen the other way round. The maximum measurable depth is restricted by the PRF:

$$P_{max} = \frac{c}{2PRF} \quad (10)$$

where  $P_{max}$ : maximum measurable depth,  $c$ : sound velocity in the fluid.

Furthermore the PRF sets a limit to the measurable velocity range. That is because of the Nyquist sampling theorem. The frequency of the signal can only be determined definitely if the sampling frequency is two times larger, otherwise frequencies are falsely assigned and aliasing occurs. That means for the PRF the maximum determinable frequency is

$$f_{max} = \frac{PRF}{2} \quad (11)$$

and according to that the maximum determinable velocity is

$$V_{max} = c * \frac{PRF}{2 * 2 * f_0} \quad (12)$$

$c$ : sound velocity,  $PRF$ : pulse repetition frequency;  $f_0$ : basic frequency.

Combining both restrictions (Equation 10 and 12) results in the constraint

$$P_{max} * V_{max} = \frac{c^2}{2 * 4 * f_0} = const. \quad (13)$$

---

That means increasing measurable depth leads to reduction of the measurable velocity range and vice versa. This constraint can be a problem if the fluid flows with high velocities and the pipe diameter is large. If measurements are done over half the pipe's diameter under these conditions the velocity cannot be determined exactly because the maximum velocity of the fluid exceeds the maximum measurable velocity and aliasing occurs.

If PRF is adjusted so that the maximum velocity can be determined instead, it might not be possible to measure across half the pipe's diameter anymore. Under these conditions it is necessary to find a compromise between measuring in great depth or to determine the maximum velocity.

The gate width is dependent on the number of cycles per pulse and the basic frequency and sound velocity

$$w = c \frac{n}{2 * f_0} \quad (14)$$

$w$ : channel width;  $n$ : number of cycles.

The velocity of the particles in every gate is calculated by

$$v = c * \frac{fD}{2 * f_0 * \cos(\theta)} \quad (15)$$

where  $fD$ : Doppler frequency.

### 4.3.3 Distortion of the spectra

In this section the causes for distortion of the spectra are explained that are visible in *Figure 8*.

The degree of distortion is dependent on the interaction of the ultrasound pulse with matter.

#### 4.3.3.1 Refraction, reflection and attenuation

In order to be able to do ultrasound imaging the presence of particles that reflect the ultrasound is essential. The concentration of particles in the fluid influences the quality of imaging. A high solid concentration reduces the penetration depth because the energy of the Ultrasound pulse is attenuated and hence not high enough to be able to supply a good signal to noise ratio at greater depth.

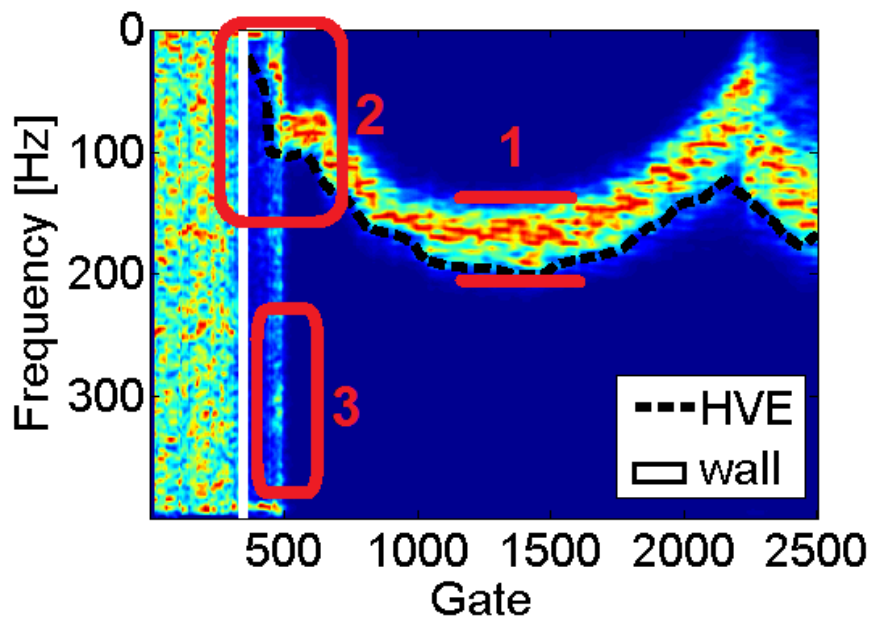


*Figure 8* Example Doppler spectrum of Oil. The higher velocity edge (HVE) and the wall position are marked. Implications that affect the profile's shape are 1: Spectral broadening. 2: Flattened profile at the wall caused by convolution. 3: Reverberation.

It has to be taken into account that refraction and attenuation change the spectral composition of the pulse and thus the mean Doppler frequency. The Doppler frequency is used for the calculation of the local velocities along the measurement axis

When the ultrasound pulse is generated it contains a bandwidth of frequencies. At interfaces the frequencies that are contained in the pulse are not equally scattered. That effect is comparable with light that is decomposed into its spectral components by a prism.

Attenuation leads to a change of the average frequency of the pulse the further it penetrates the material. Higher frequencies are more attenuated than lower ones. All these effects were theoretically investigated among others by Embree, 1990.

Another parameter that is important to take into account for estimating the correct velocity is the change of incident angle after refraction at interfaces, e.g. liquid wall interface.

### 4.3.3.2 Spectral Broadening

There are several effects that cause broadening of the spectrum that can be seen in *Figure 8*. First of all the change of amplitude of the pulse when it is generated makes it impossible to determine the original excitation frequency exactly. The spectrum of the pulse is already broadened and hence the reflected signal will also have a broadened spectrum which is modulated by the limited observation time as well.

Additional broadening effects have the different paths a particle can take to cross the sampling volume. Not all the particles move perfectly parallel to the flow direction.

If a particle travels over the pulse's cross section the reflected signal will first have low amplitude then reach a maximum and decrease again. This leads to broadening of the spectrum (see *Figure 9*). This is called the transit time broadening (Yu, 2006).

Furthermore, the movement of the particle does change the geometric relations between the transducer and the particle, the distance between them changes and hence the Doppler angle which leads to a wrong velocity estimation using Equation 15 (Green, 1964).

If it was only one particle in the fluid it would be possible to correct for these effects in the velocity estimation algorithms, however, all particles contribute and make a correction very difficult. The signals from all the particles contribute and they interfere constructive and destructive. The resulting power spectrum is shown in *Figure 10*. It is more difficult to locate the true max intensity frequency.

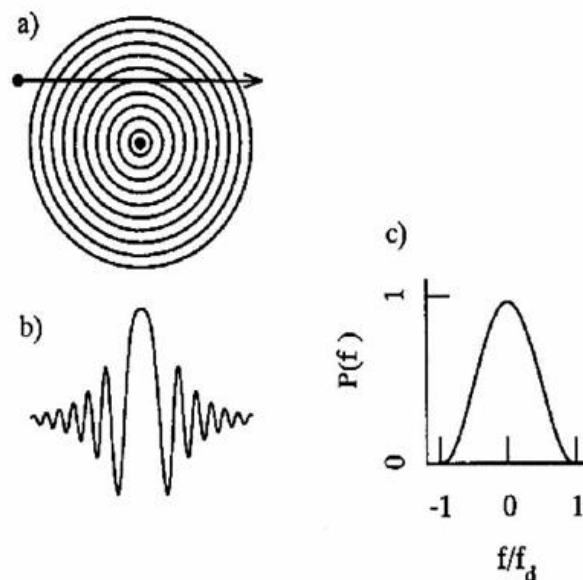


*Figure 9* a) A particle travels across the pulse's cross section. b) The change of intensity over the pulses cross section leads to a signal with changing amplitude. c) The change of amplitude and the change in Doppler angle relative to the transducer lead to broadening of the spectra, (Jones, 1993).

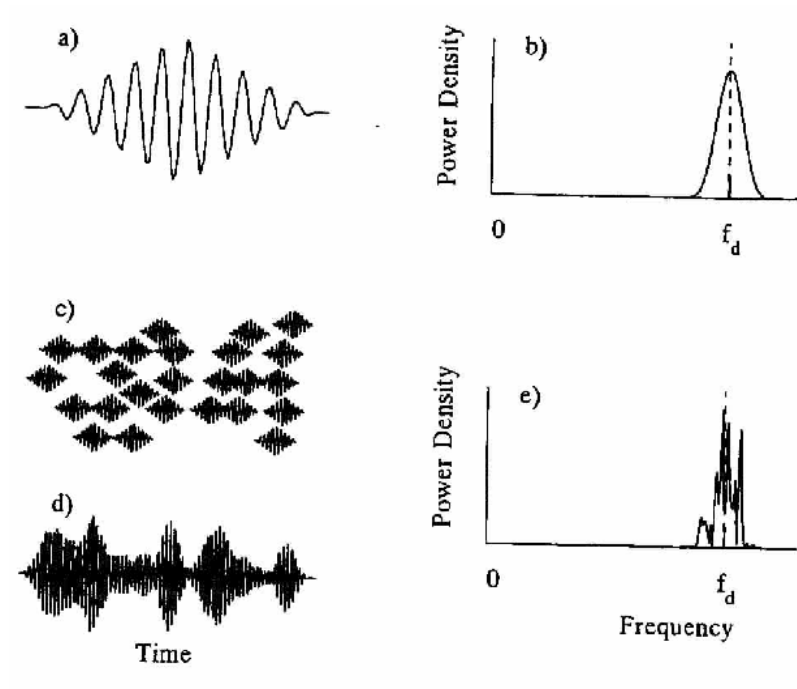


**Figure 10** Effect of multiple scatterer on the estimated Doppler spectrum. The signal from a single particle a) has a smooth spectrum b) Signals from multiple particles c) are summed d), the result has a spectrum with sharp peaks e), (Jones, 1993).

### 4.3.3.3 Convolution

Because of the spatial extension of the pulse it is the mean velocity of all particles within the pulse that is estimated. The region that the pulse covers is called sampling volume.

The measured velocity profile can be mathematically described as the convolution between sampling volume and velocity profile.

The convolution process is illustrated in *Figure 11*. The distortion is especially strong if the sampling volume overlaps with the wall, where the velocity is zero, and the flowing fluid as can be seen in *Figure 11 a), b), d), e)*. The measured velocity profile is flattened at the edges. This can also be seen in *Figure 8*, region 2).

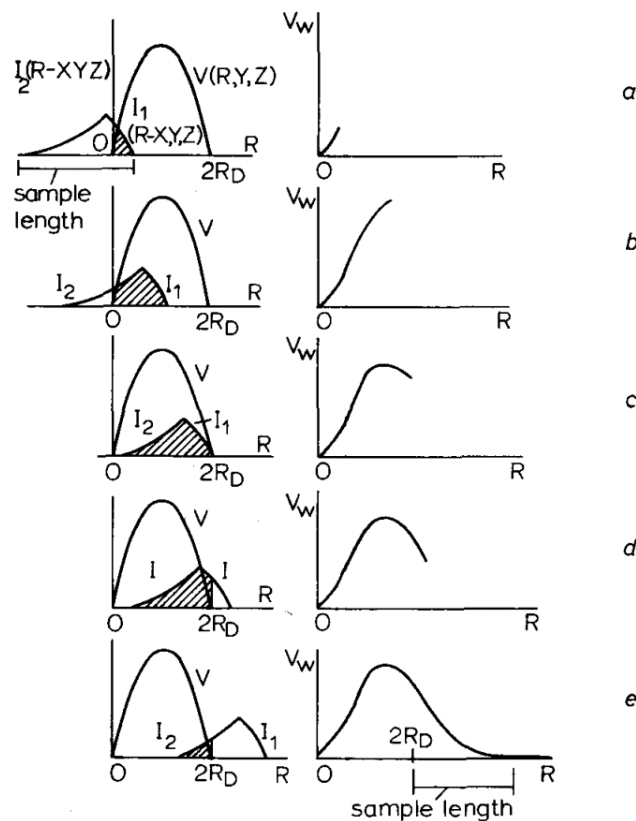


*Figure 11* Illustration of convolution of sampling volume and velocity profile. Left: Overlap of sampling volume and velocity profile  $V$ . Right: Measured velocity profile, (Jorgensen, 1973).

#### 4.3.3.4 Reverberation

Region 3 in *Figure 8* shows an artifact of multiple reflections within the stainless pipe. This ultrasonic artifact is called reverberation (Huang, 2007) and causes a mirror image of the wall in the spectrum at greater depth.

The concept of reverberation is shown in *Figure 12*. The reflection increases the time until the transmitted signal returns to the transducer and hence gives the impression of the interface being at a greater depth.

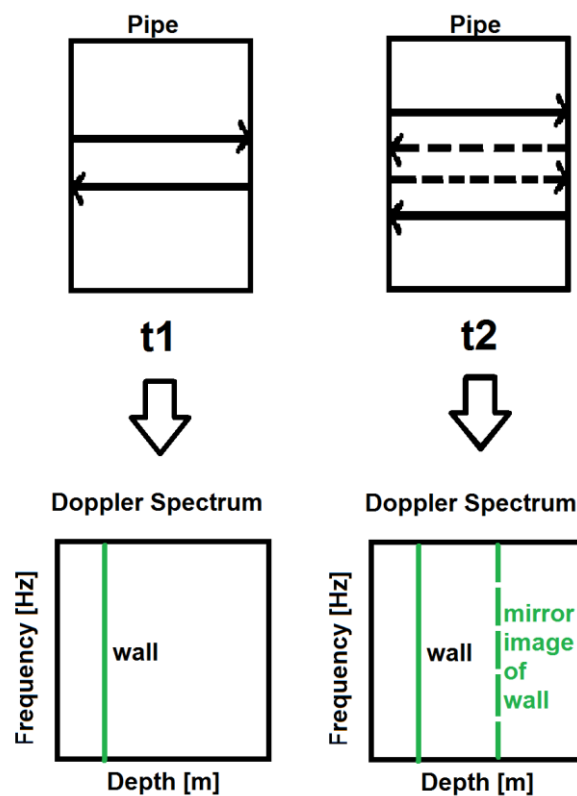


*Figure 12* Illustration of reverberation. Because of multiple reflections between the pipe walls (right) the time until the pulse returns to the transducer is increased and a mirror image of the wall is visible in the image.

### 4.3.4 Measurements with Flow-Viz™

Measurements of the flow of the fluid were done with Flow-Viz™ a fluid characterization system that was developed at SIK<sup>4</sup> and CPUT<sup>5</sup>. The fluid is pumped through a flow-loop that is built up out of a tank that contains the fluid, a pump, a pipe line and Flow-Viz™.

Flow-Viz™ incorporates the non-invasive in-line sensor unit, an operator's panel with electronics for data acquisition and signal processing and software for signal processing (Figure 13, left).

The sensor-unit is easily integrated into the pipe line because of its compact design (Figure 14). It is built up out of a transducer mounted to a wedge. Wedge and coupling media allow the contactless measurement of the velocity in the pipe and they are needed to prevent the near-field of the transducer to overlap with the measuring window. The acoustic impedance of wedge and coupling medium are known. Thus the change of angle caused by refraction at interfaces with different impedance can be taken into account. The wedge and sensor unit is designed in a way so that the Doppler angle is 20° inside the pipe.

For the measurement the fluid is pumped from the tank into the pipe line. The actual measurement is conducted in the sensor unit. The transducer switches repeatedly between transmitting and receiving mode with the pulse repetition frequency. The data is acquired and available for further processing with customized velocity profile estimators. The experimental set-up and the methodology are described in more detail in (Kotzé R. a., 2013) and (Flow-Viz, 2014).

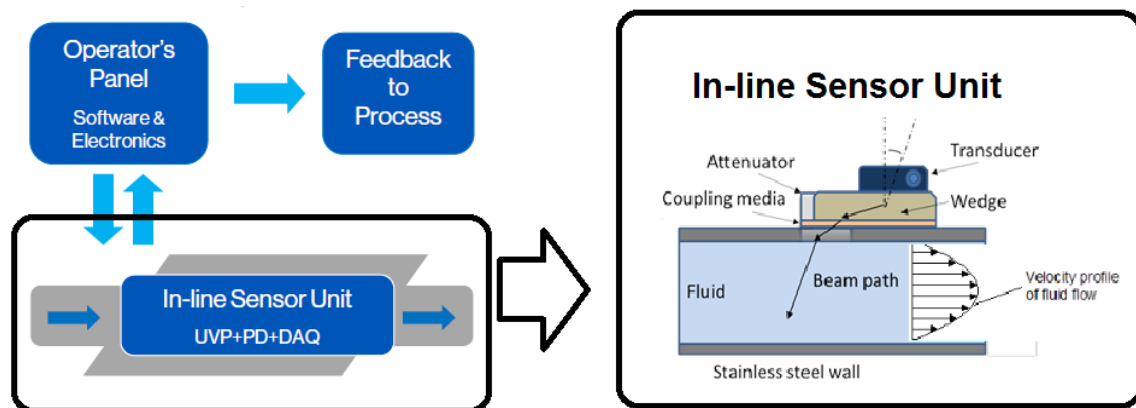


Figure 13 Schematic illustration of the experimental set-u, (Flow-Viz, 2014).

<sup>4</sup> SIK- The Swedish Institute for Food and Biotechnology

<sup>5</sup> Cape Peninsula University of Technology



Figure 14 Picture of Sensor-unit of Flow-Viz.



## 5 Image based velocity profile estimation

In this chapter the image based velocity profile estimator will be described. The code written in MATLAB consists out of three main parts:

1. Signal progressing
2. Wall detection
3. Velocity profile detection.

### 5.1 Signal processing

As a first step the data has to be converted into a power spectrum (Doppler spectrum) which is visualized and serves as the basis for the image processing.

Starting point is the raw data from the measurement. The raw data consists out of in-phase (I) and quadrature/Co-phase (Q) signal. The Q signal is 90° phase shifted to the I signal. I/Q signal contains directional information of the flow. The I and Q signals are acquired in a matrix  $iq$  with the dimension (Number of pulse repetitions) x (Gates) x (Number of profile blocks).

*Figure 15* serves as a good illustration of the next steps. For every single gate (the vertical dotted line marks the position of one gate):

- The mean over the amplitudes of every pulse is calculated.
- The mean is subtracted from every single pulse amplitudes ( $iq(gate) = iq(gate) - mean(iq(gate))$ )
- That leads to a similar signal as shown in the right graph in *Figure 15*. This is done for the Co-phase and In-phase signal.
- The resulting signal is multiplied by a hamming window. The hamming window reduces spectral leakage.
- Co-phase (cp) and the in-phase (ip) signal are combined to a complex signal:  $Y = iq - i * cp$  where  $i$ : imaginary unit.
- Fast Fourier Transform is performed. The result is a frequency spectrum which is used to calculate the normalized power spectrum  $PS = (FFT(Y))^2 / max(FFT(Y))$
- Not assigned numbers that might occur after the previous step are set to zero.

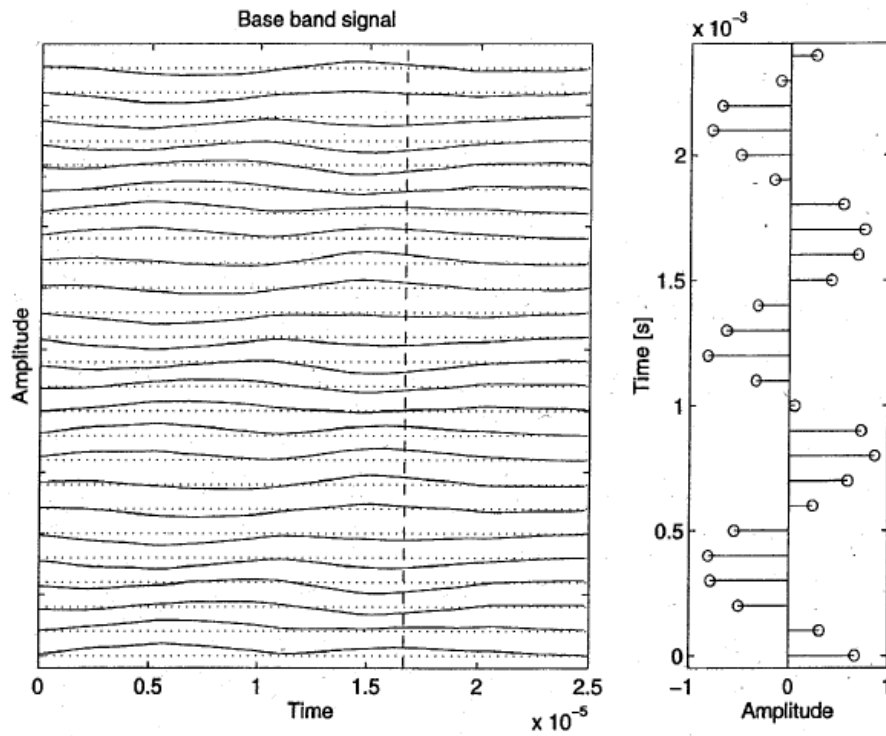


Figure 15 Left: Profile block. The time axis corresponds to physical depth. The dotted line marks the position of one gate. Right: Change of amplitude of pulses at one gate.

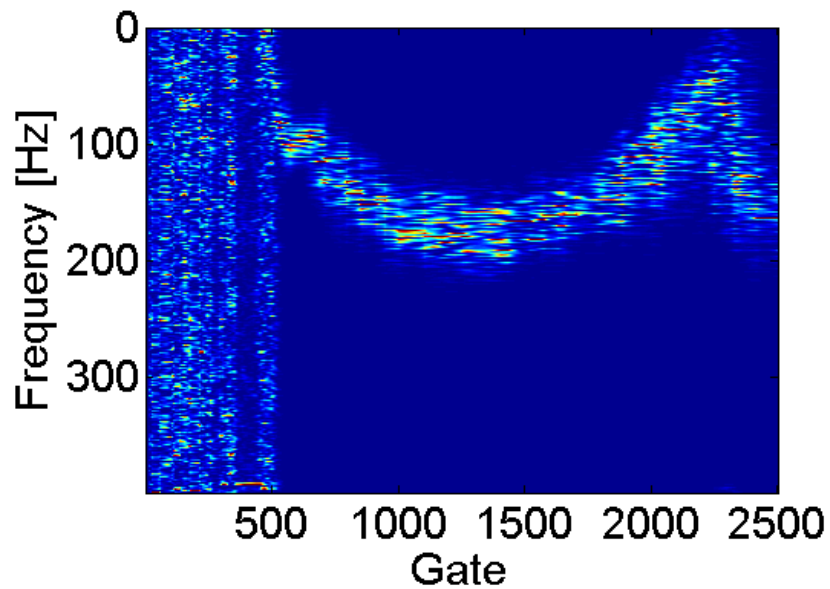
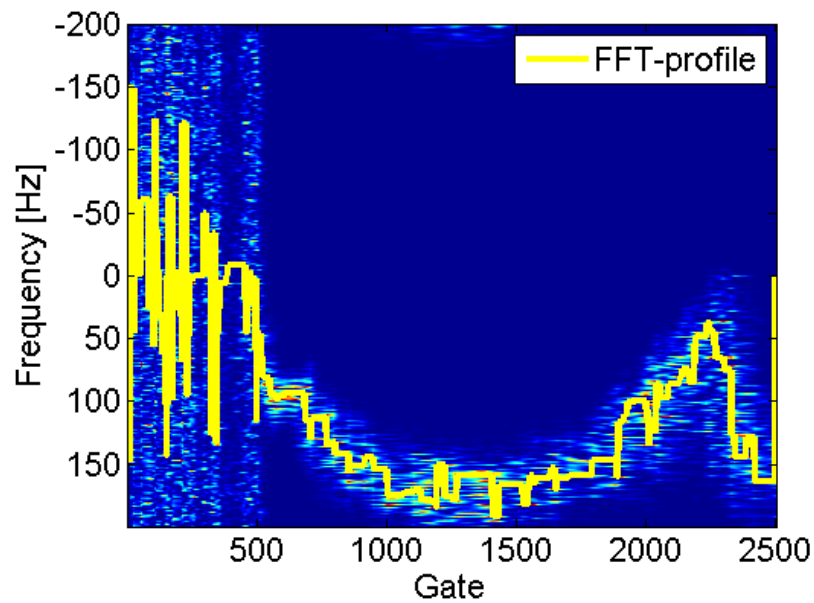
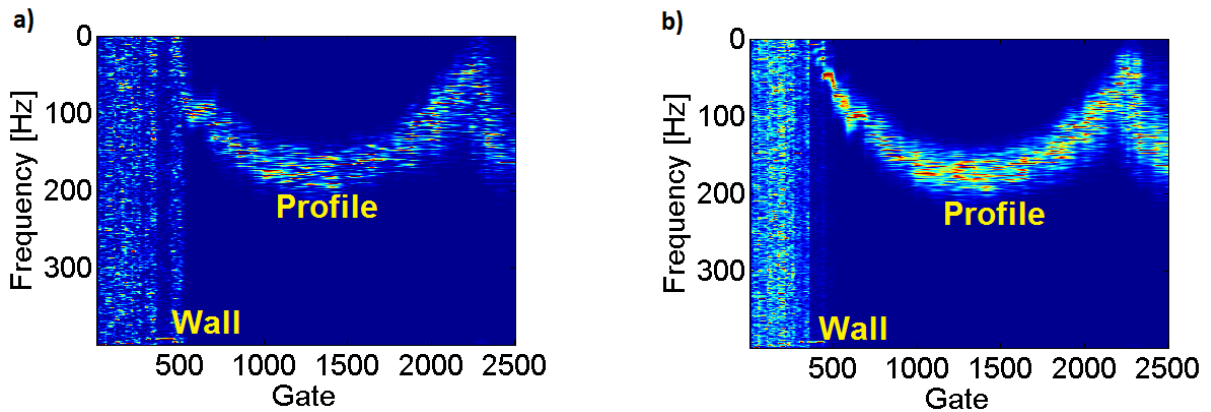


Figure 16 Doppler spectrum of oil. One profile block with 512 pulse repetitions was used.



*Figure 17* Doppler spectrum (512 pulse repetitions) with FFT- profile. At every gate the frequency with the highest intensity value is chosen as profile point.

That is the basic procedure to end up with a power spectrum (Doppler spectrum) that can be displayed (*Figure 16*) and is the basis for the image based velocity profile estimator. The old frequency based velocity estimator algorithm continues from this point by using at every gate the frequency coordinate with the highest intensity and calculates the corresponding velocity. The velocity profile that originates from this procedure is labeled as "FFT- profile" (*Figure 17*).



*Figure 18* A) Doppler spectrum using 512 pulse repetitions and one profile block. B) Doppler Spectrum using 4 profile blocks with 512 pulse repetitions each.

Instead of using only one profile block for generating the Doppler spectrum it is possible to calculate the Doppler spectrum of several profile blocks and then calculate the average. As can be seen in *Figure 18* the profile and wall position are clearer if more profile blocks are used. The effect of using more profile blocks onto the wall detection, the profile's shape and processing time will be discussed in Section 6.2.3.

The next step is to correct the image for aliasing if aliasing is present. If the frequency range is not wide enough frequencies that exceed the frequency range are falsely assigned. The frequency range is exceeded if the flow velocity is higher than the maximal measurable velocity (see Section 4.3.2).

In order to correct the image the frequency coordinate that corresponds to frequency 0 Hz is determined.

The part of the image from the zero frequency coordinate to the bottom is shifted to the top of the corrected image and the upper part of the image is shifted to the bottom (compare *Figure 19*).

The correction is similarly done for the frequency array and the velocity array. However, instead of shifting the upper part of the frequency array down the frequency array is filled up with continuously increasing frequencies.

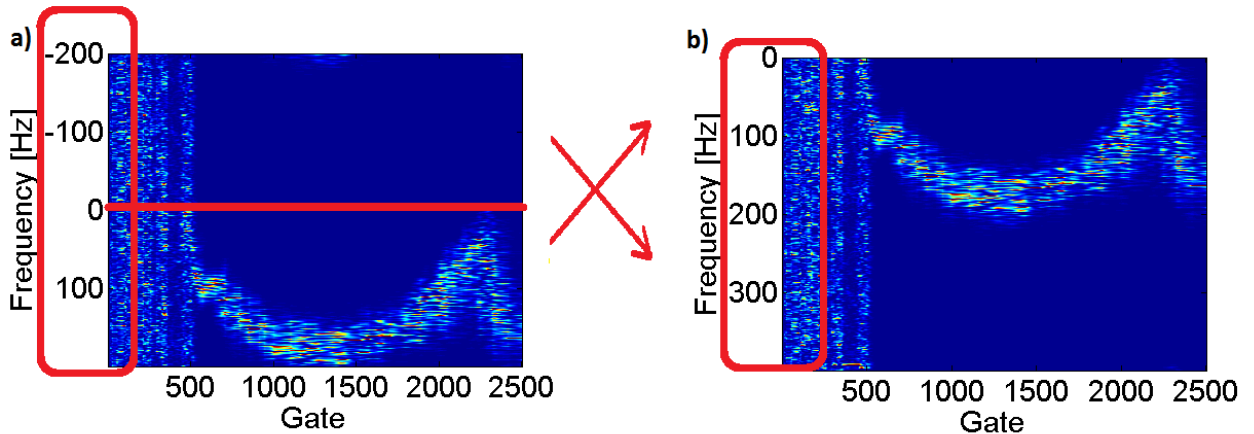


**Figure 19** Illustration of correction for aliasing. The lower part of the image is shifted to the top of the corrected image b) while the upper part is shifted down. The frequency array is extended. The number of pulse repetitions per profile was 512.

After correction for aliasing the image is interpolated along the vertical axis.

The interpolation of the image is an important step, especially if a low number of pulse repetitions are chosen, because the interpolation will increase the resolution of the image.

It is preferable to use a low pulse repetitions number because that reduces the processing time. However, if a low pulse repetitions number is used the flow profile's shape is very pixelated as can be seen in *Figure 20*.

The image with the dimension (n x m) is interpolated by an interpolation factor. The result is an image with the dimension (n\*interpolation factor x m). That means to increase the frequency array's resolution (*Figure 20, a*). The interpolation factor was chosen so that the vertical dimension equals 512 pixels. This value is a good compromise between image quality and computational time. The velocity array has to be interpolated as well. It is not necessary to interpolate the image along the gate axis because the resolution is already high (e.g. over 2000 gates for a 2 inch pipe).

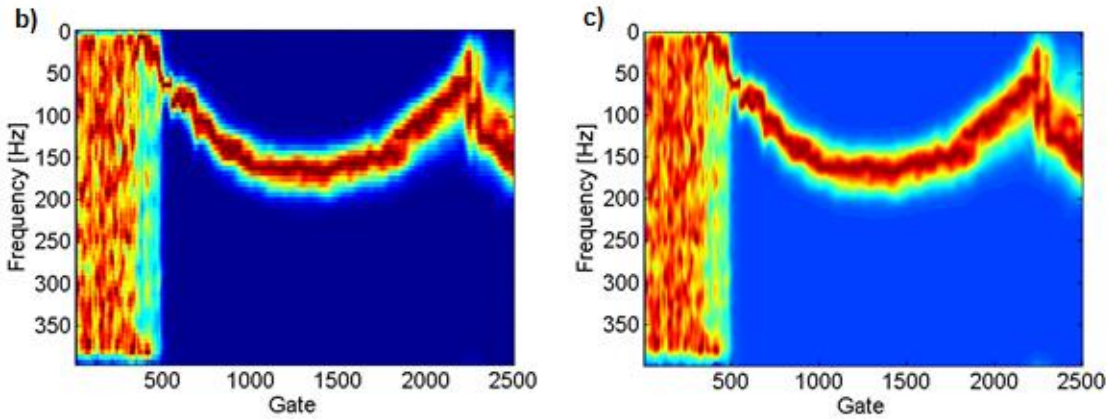
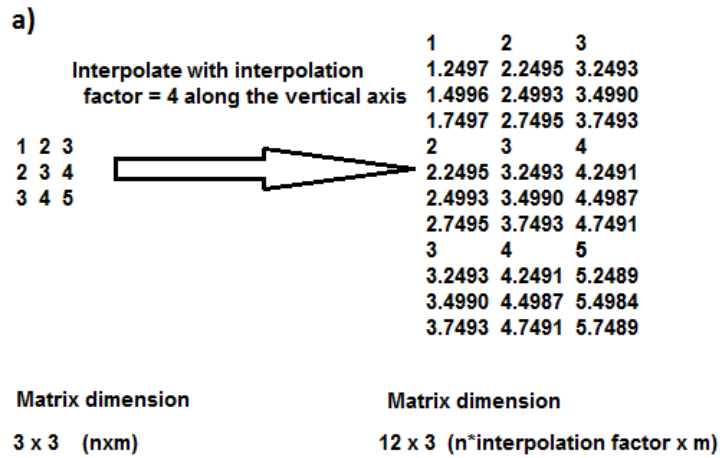


**Figure 20** Illustration of interpolation step for a Doppler spectrum with 64 pulse repetitions. The average over 32 profile blocks was calculated. A) The dimension of the profile block in vertical direction is extended by the interpolation factor. The resolution of the frequency array increases. The result is a smoother flow spectrum. B) Flow spectrum with 64 pulse repetitions. C) Flow spectrum after interpolation of the vertical axis from 64 pixels to 512 pixels.

The next step is application of an image averaging filter. The averaging filter is a linear spatial filter (Chodorowski, 2014). If the filter has the dimension  $N \times M$  where  $M = 2a+1$  and  $N = 2b+1$  and  $a, b$  are positive integers and the image has the dimension  $(n \times m)$  with the old image pixel  $f(x, y)$  the new pixel value is calculated as

$$g(x, y) = \sum_{s=-a}^a \sum_{t=-b}^b w(s, t) f(x + s, t + t)$$

$w$ : is the filter mask given as

$$w = \frac{1}{N * M} * (N \times M \text{ Identity matrix}).$$

The effect of the averaging filter is illustrated in *Figure 21*. The size of the averaging filter is chosen to be about 0.05% of the dimension in each direction. That means 25 pixels in vertical direction if the number of pixels is 512 in total and 100 pixels in horizontal direction if the number of gates is 2500.

The averaging filter is a smoothing filter, thus the profiles edges are smoothed and weight of noise is reduced (see *Figure 22*).

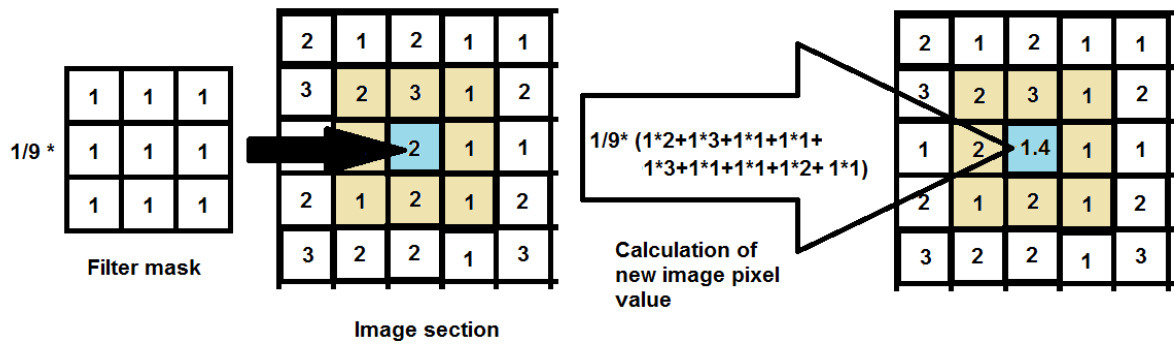


**Figure 21** Illustration of averaging filter. The filter mask is applied onto the image pixel (blue). The average of all pixels that are covered by the filter mask (yellow) is calculated and used as the new image pixel value.

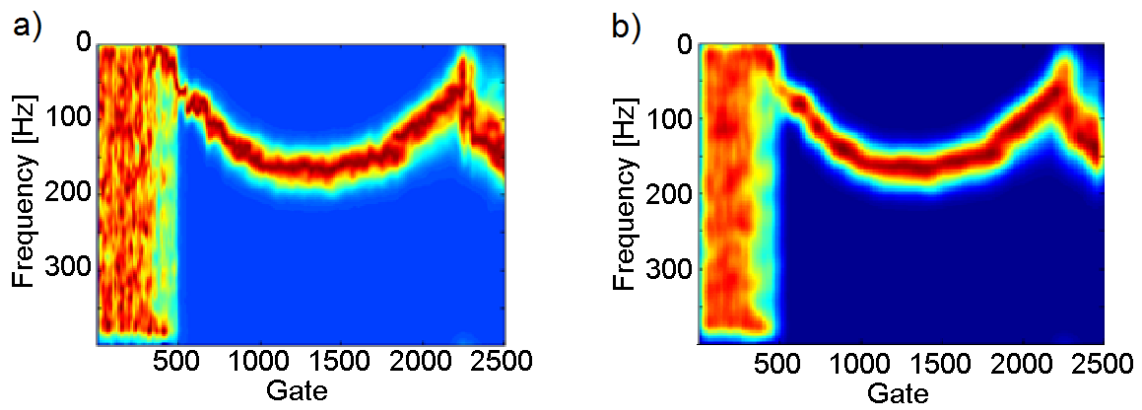


**Figure 22** Comparison of image before a) and after b) the application of the averaging filter. The profile is smoothed and noise (close to the wall) is reduced. The number of pulse repetitions was 64 and 32 profile blocks were averaged to generate the Doppler spectra.

## 5.2 Wall detection

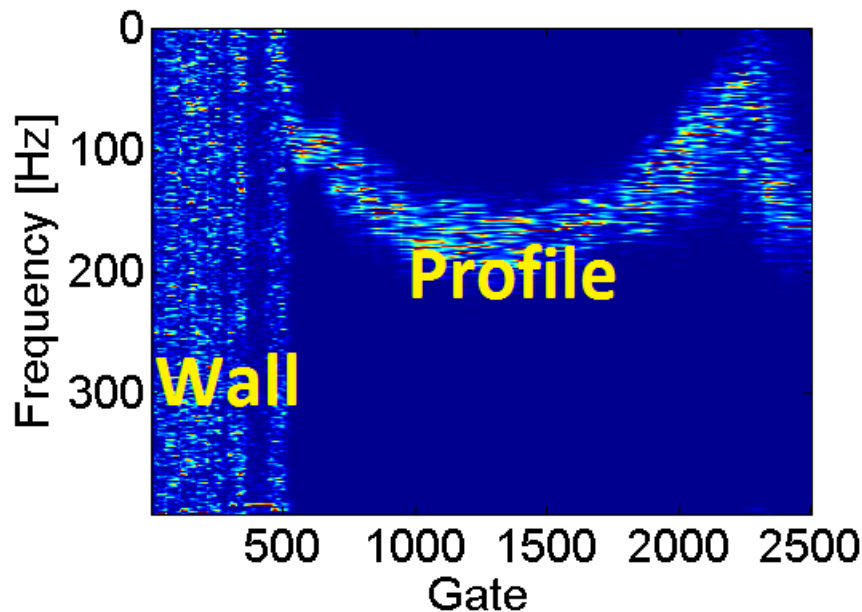


*Figure 23* Illustration wall position and profile. The wall is visible as a static signal.

The second part of the code is responsible for the wall detection. There are walls on both sides of the pipe. However, the signal on the far side from the transducer is often not applicable because of attenuation and noise. Therefore only the wall close to the transducer shall be considered and detected (see *Figure 23*). In the image the wall is visible as a stationary signal for that reason it covers the whole frequency range.

The wall detection works as follows:

1. Generate binary image according to threshold intensity value. Binary images can only have two possible values. In this case pixels with intensity values higher than the threshold intensity value are set to one and all the others pixels are set to zero.
2. Apply image filters (erase small artifacts, close gaps)
3. Wall extraction and determination of the wall gate coordinate.

---

### Step 1: Generate binary image

There are two alternative ways for finding the threshold value. Either it is found automatically by a MATLAB function or it is possible to preset a certain ratio of the image pixels that should be erased.

The first step for both approaches is to generate a histogram of the image intensity values. The automatic function finds the best threshold value in order to separate the foreground intensity distribution from the background distribution (see *Figure 24*). Depending on the image quality (e.g. high level of noise) it might be better to keep another ratio of pixels; which can be manually set.

The threshold intensity value is used to generate the binary image (*Figure 26 a*). The effect of different manually chosen ratios will be discussed in Section 6.2.1.

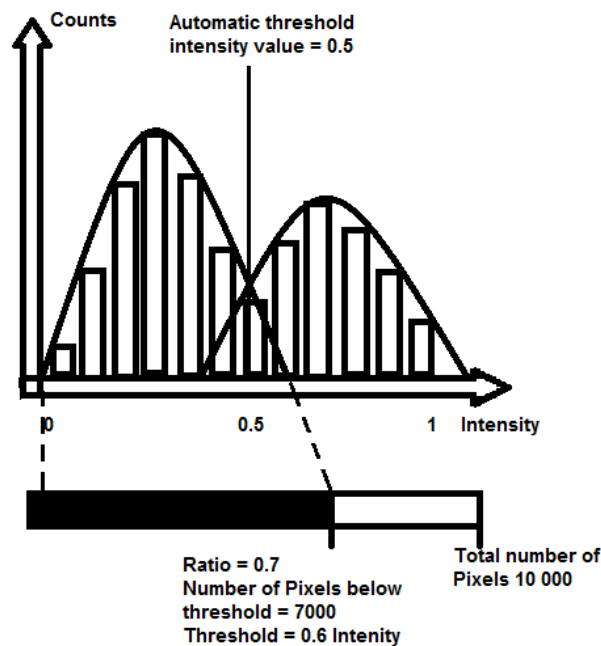


*Figure 24 Find threshold intensity value. The automatic MATLAB function determines the threshold intensity value that separates the foreground and background distribution the best. The manual threshold finds the intensity value that erases the number of pixels according to the preset ratio.*

**Step 2: Apply image filters**

After generating the binary image (*Figure 26 a*) it is necessary to remove artifacts from it. Image parts that are smaller than a certain pixels size are removed. The pixel size must not be too small in order to remove as many noise artifacts as possible but it must not be too large either. Important information might be removed otherwise.

Furthermore, vertical gaps are closed with the help of a closing filter. Closing is necessary to be able to extract the wall in the next step and because the wall edge is quite noisy (compare *Figure 26 a*) and b)). The operating principle of the closing and opening filters is illustrated in *Figure 25*.

The filter shape and size can be chosen. The closing filter closes gaps and the opening filter removes parts that are smaller than the filter size.

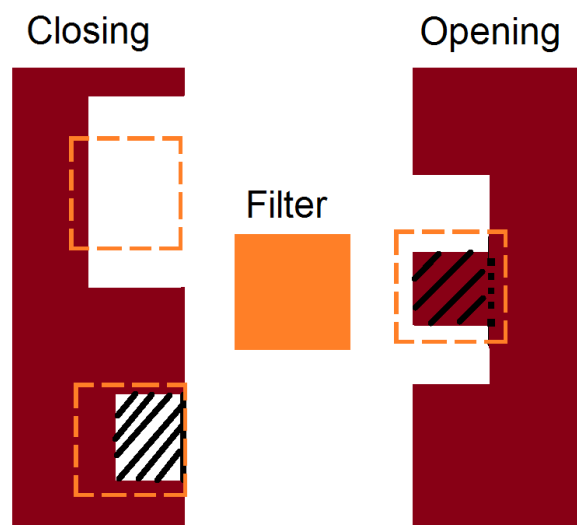


**Figure 25** Illustration of closing and opening filters. Closing: The filter closes gaps that are smaller than its size. Opening: Removes parts that are covered by the filter.

### Step 3: Wall extraction and determination of the wall gate coordinate

A rectangular opening filter is used that removes everything in the binary image except for vertical lines that go all the way from the top to the bottom of the image (*Figure 26 c*) The vertical right edge of the remaining wall is detected with an edge detection filter and is determined as wall gate (*Figure 26 d*). The distance between the gates is calculated by

$$gate\ distance = \frac{1}{2 * sampling\ frequency} * c \quad (16)$$

With  $c$ : velocity of sound. Knowing the pipe radius  $R$  and the Doppler angle  $\Theta$  the number of gates from the wall gate coordinate to the center gate can be estimated as

$$no\ gates\ to\ center = \frac{R}{\theta * gate\ distance} . \quad (17)$$

It is necessary to know the center of the pipe if the velocity profile cannot be determined over the whole cross section of the pipe because of attenuation. It is enough to know half the velocity profile to be able to determine the rheological properties and the volumetric flow rate of the fluid.

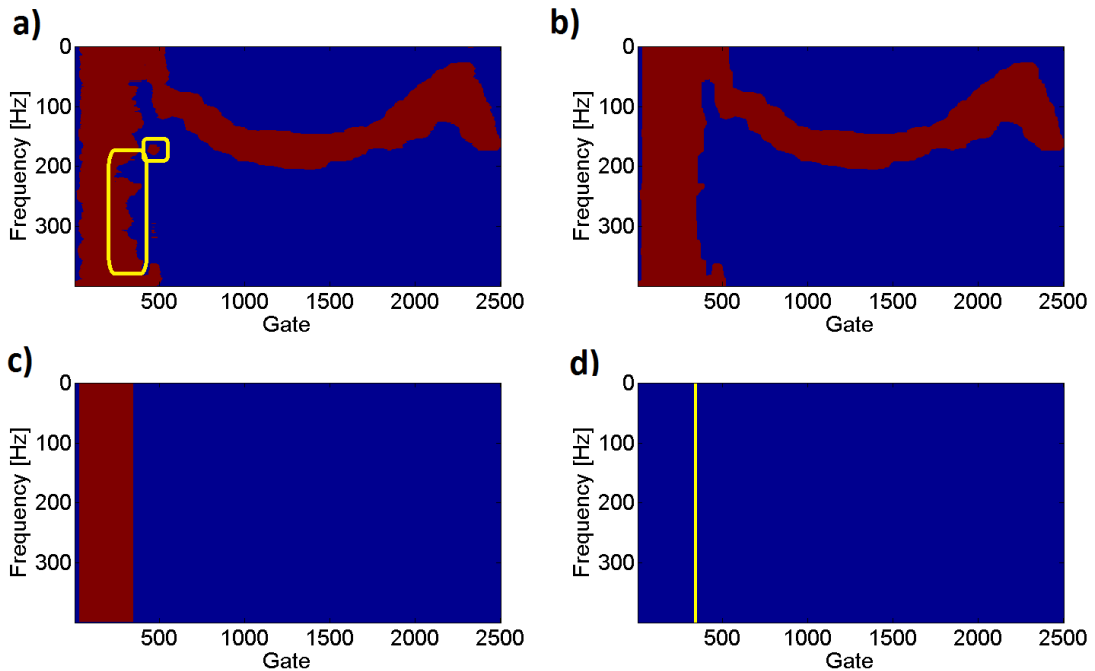


*Figure 26 a) Binary image after thresholding. b) after application of image filters. Observe closing of gaps at the wall and removal of noisy artifacts c) wall extraction d) determination of wall gate coordinate.*

## 5.3 Profile detection

The steps for profile detection are as follows:

1. Generate binary image according to threshold intensity value (set pixels with intensity values higher than the threshold to one and all the others to zero).
2. Apply image filters (erase small artifacts)
3. Horizontal edge detection
4. Rescaling
5. Calculation of velocity profile.

The process for generating the binary image is the same as for wall detection (Section 5.2). However, after the binary image is created only noisy artifacts are removed because the profile shape shall be conserved and not be modified by opening or closing operations.

An edge detection filter finds the horizontal edge on the higher velocity side of the flow profile as can be seen *Figure 27 b*), called Higher Velocity Edge (HVE).

The frequency at the center gate of HVE is rescaled to the frequency with the highest intensity as illustrated in *Figure 28* and the velocity is calculated using *Equation 15*. After rescaling it is possible that some frequency values might exceed the frequency range. In that case these values are set to zero.

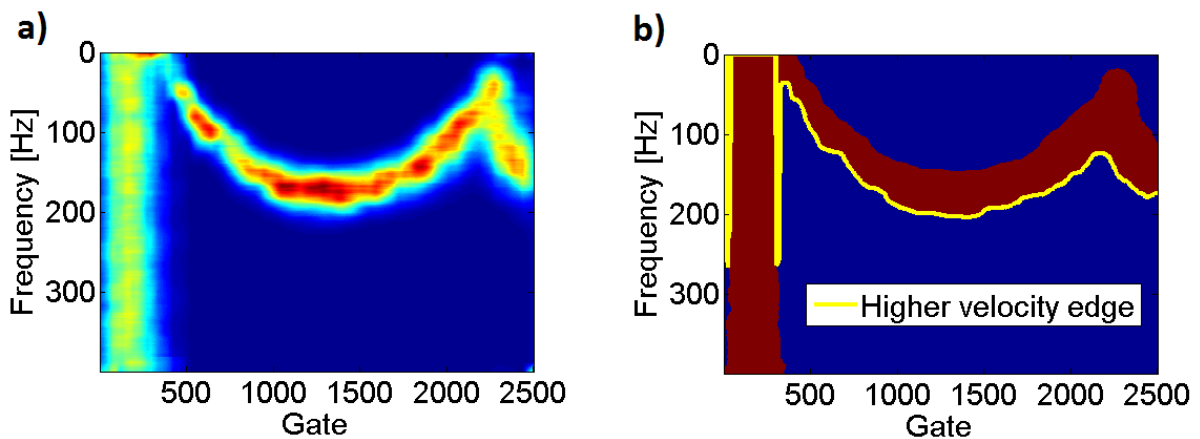


*Figure 27* Detection of higher velocity edge. a) Image using 512 pulse repetitions and 4 profile blocks after averaging filter. b) Binary image after thresholding and detection of higher velocity edge.

---

A prominent feature in *Figure 28* is the peak in the profile close to the wall. The wall edge in the binary image is not perfectly straight, because of that a few coordinates of the wall edge are falsely detected as part of the profile.

Another artifact that originates from following the outer edge of the profile is that the velocity seems to increase at the wall. These artifacts can be more or less significant depending on the image's quality. In order to correct for this the following profile detection functions: were developed

1. Use both edges (BE)
2. Prevent increase of velocity (PIOV)
3. Correct steps

These options are manually selected by the user.

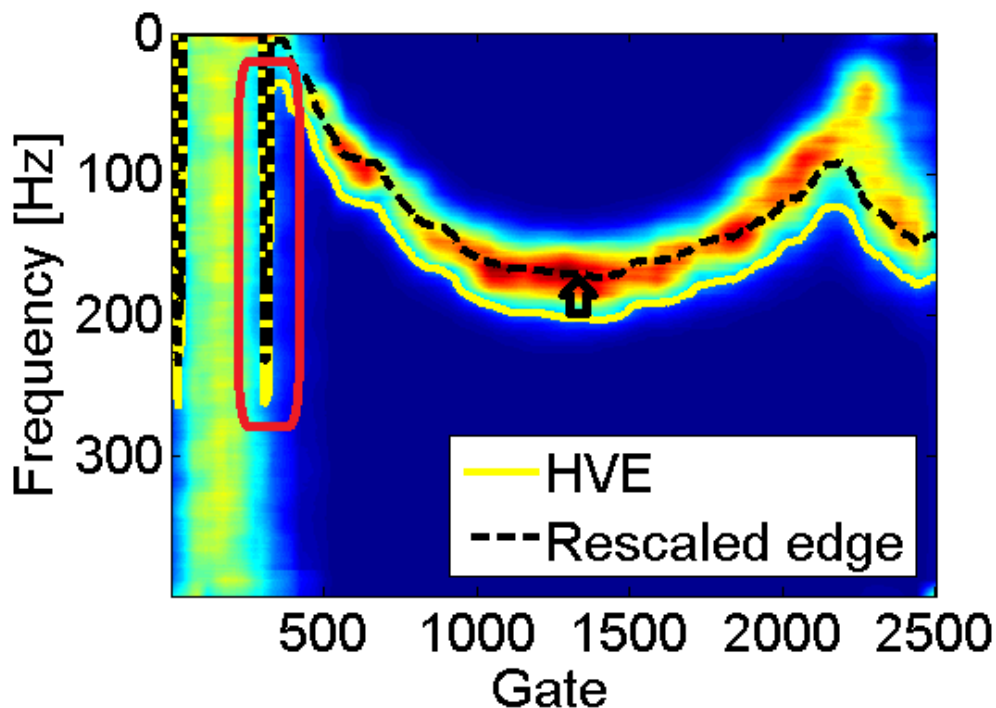


*Figure 28* Rescaling of the higher velocity edge (HVE). The frequency of the HVE at the center gate coordinate is rescaled to the frequency with highest intensity in the image. The image was obtained using 512 repetitions and the average over 4 profile blocks. Marked is the part of the profile that exhibits increase of velocity and falsely assigned wall edge parts that lead to the prominent peak in the profile's shape.

### 5.3.1 Use both edges (BE)

If this option is chosen the Lower Velocity Edge (LVE) is detected additional to the Higher Velocity Edge (HVE).

LVE is detected by the same horizontal edge detection filter as HVE except for that the filter is flipped upside down. The lower velocity edge is rescaled to the frequency with the highest intensity at the center gate and then the average of both rescaled edges (HVE rescaled + LVE rescaled) is estimated (Figure 29). From the average of both edges the velocity is calculated using Equation 15.

Summary of steps for BE:

1. Detect higher velocity edge
2. Rescale higher velocity edge
3. Detect lower velocity edge
4. Rescale lower frequency edge
5. Compute average of rescaled edges
6. Calculate velocity profile

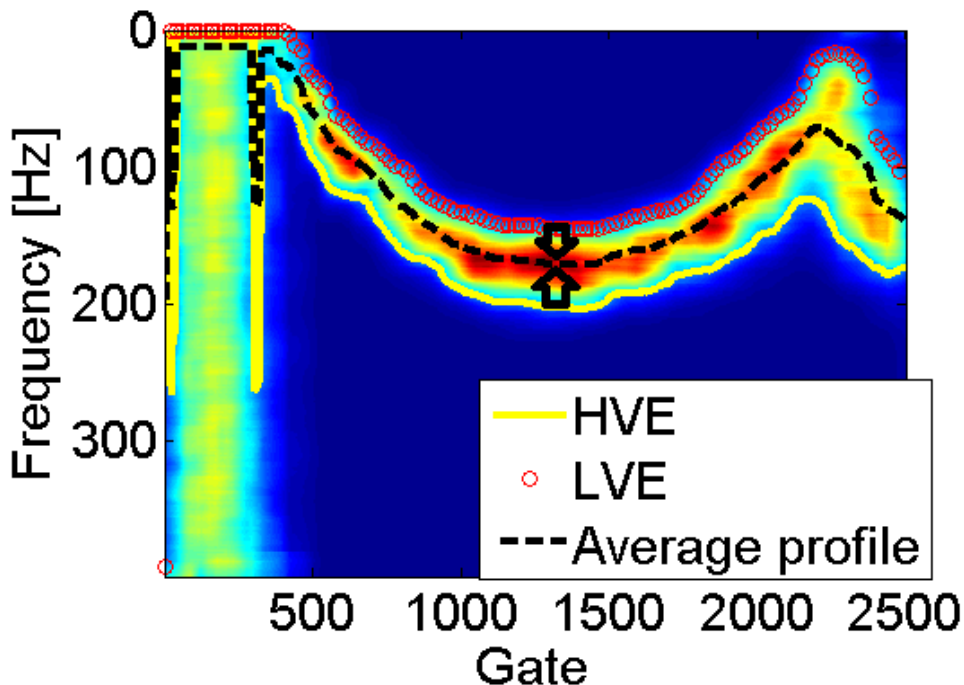


Figure 29 Rescaling of both profile edges. The average is used for the velocity estimation.

### 5.3.2 Prevent increase of velocity (PIOV)

This option prevents the increase of velocity at the wall and interpolates the profile from the position, where the velocity starts to decrease, to the wall instead. If this function is enabled it is applied to both edges; the higher and the lower velocity edge. It can be reasoned that this procedure is appropriate because theoretically the velocity can be different from zero because of wall slip but it cannot increase at the wall.

Summary of steps for PIOV:

1. Remove strong abrupt changes in the edge
2. Find the position where the frequency starts to increase
3. Interpolate from that point to the wall.

First abrupt and strong changes in the respective edge are found by scanning the edge backwards from the center gate to the wall gate and compare the consecutive frequency values. Extreme values are replaced by the frequency value of the previous gate.

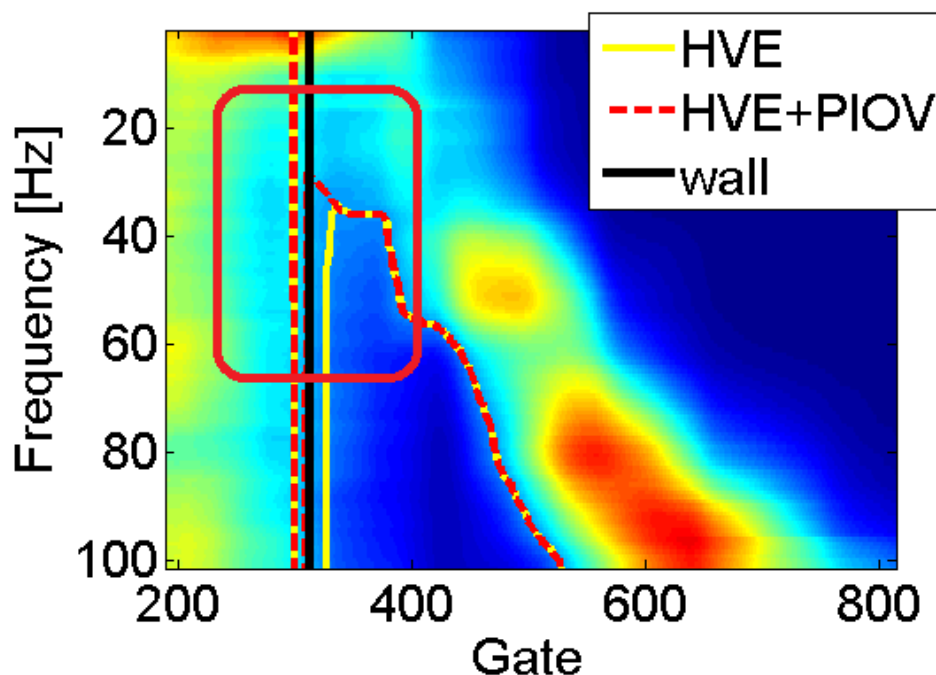


*Figure 30 Prevent increase of velocity at the wall (PIOV). The higher velocity edge after the application of PIOV does not follow the profile's outer edge close to the wall. Instead the profile is interpolated to the wall.*

After the removal of abrupt changes the edge is scanned forward starting from the wall gate coordinate. The gate coordinate of the edge where the frequency starts to increase after it was decreasing (turning gate coordinate) is found. From the turning gate coordinate the edge is interpolated back to the wall. The slope that is chosen for the interpolation is the mean slope from the turning gate and continued over a certain range (ca. 10% of the total number of gates).

One example can be seen in *Figure 30*. Instead of that the velocity increases at the wall it decreases.

### 5.3.3 Correct steps in the profile shape (CS)

Steps in the profile can be due to distortions of the profile or the application of PIOV that removes strong abrupt changes in the edge. The steps can be corrected as follows:

1. Differentiation of the profile
2. Find steps
3. Determine the step width.
4. Correct Step.

The derivative of the profile has high values at the steps position (*Figure 31*). That is how the steps are found. Then the function scans the adjacent gate and compares the slope of the narrow environment of the step with the slope of a wider region (illustrated in *Figure 32*). Because the slope of the flow profile changes across the diameter of the pipe it is not possible to choose the slope over the whole profile as a measure of reference.

If the slope is smaller than 0.7 percent or bigger than 1.3 percent of the mean of the wide range, the adjacent gate is added to the step width. If the step width is found, the step edges are connected and in this way corrected (see *Figure 33*).

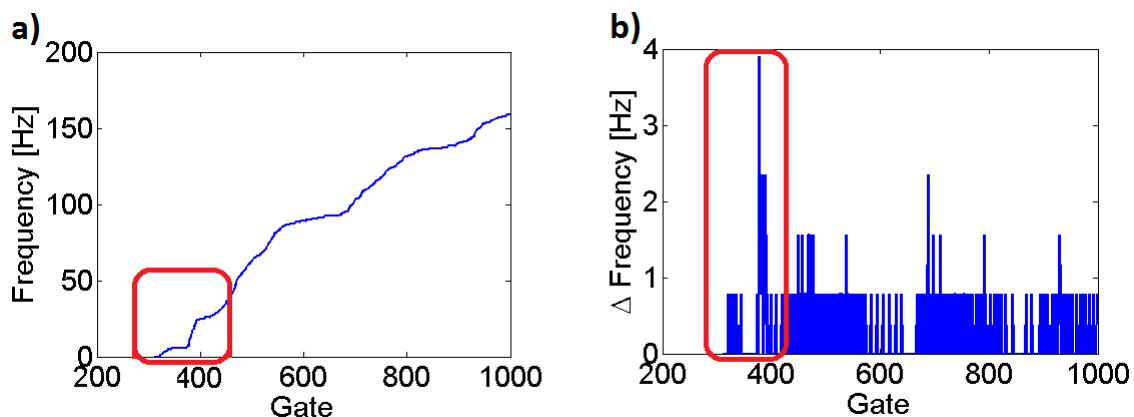


*Figure 31* Left: Image-profile with steps originating from the application of PIOV. Right: Derivative of the profile. The steps in the profile are detected by the high values of the derivative.

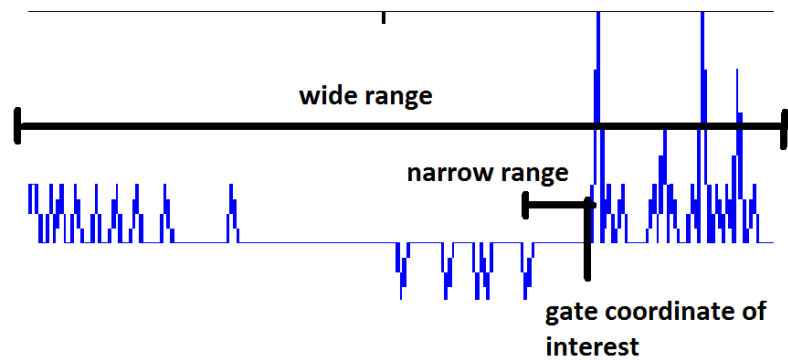


*Figure 32* From the step (which had a very high derivative value) the width of the step is determined by scanning the adjacent gate coordinates. The slope of a narrow range around the gate coordinate of interest is compared with the slope of a wider range of the profile.

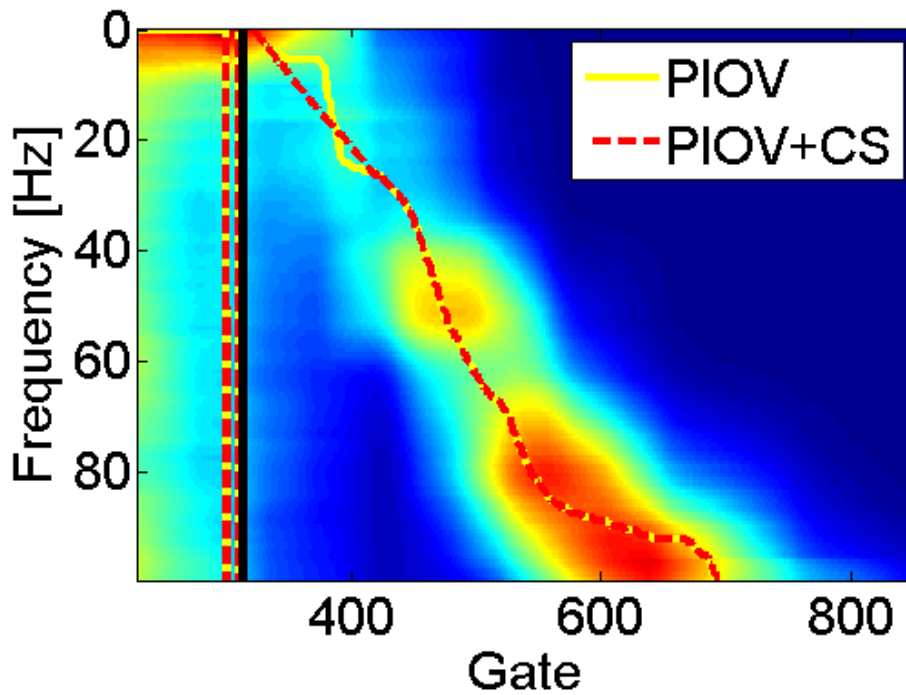


*Figure 33* Steps in the profile that are apparent after edge detection are corrected by the Correct Steps function. The profile follows a shape that is theoretically more reasonable.

---

# 6 Evaluation of image based velocity estimator

This chapter concerns the evaluation of the image based velocity estimator described in Chapter 5.

The main aspects that are used for the evaluation of the velocity estimator are

1. Processing time
2. The reliability of wall detection
3. The shape of the velocity profile and resulting rheology estimates

In Section 6.1 the image based velocity estimator is tested on a simulation in order to get a first impression of how well the velocity estimation of the image based velocity estimator could work.

Furthermore the image based velocity estimator is evaluated using real measurement data. The influence of different parameter settings and the results are discussed in Chapter 6.

## 6.1 Test on simulation

### 6.1.1 Description of simulation

The simulation is a modified version of the Doppler signal simulation, 21.Sept.02, by Hans Torp, Norwegian University of Science and Technology.

It demonstrates one point particle in solution moving across the pipe width. Its velocity is increasing till the middle of the pipe and then decreasing again.

It can be chosen whether the velocity profile across the pipe has a parabolic or flat shape (*Figure 34*).

The pipe wall is simulated by another particle that is randomly moving back- and forward in a small restricted area at the beginning of the velocity profile. The particle has to move randomly in order to detect movement and generate frequencies over the whole available frequency range.

The advantage with the simulation is that one knows exactly the particle's velocity at every position.

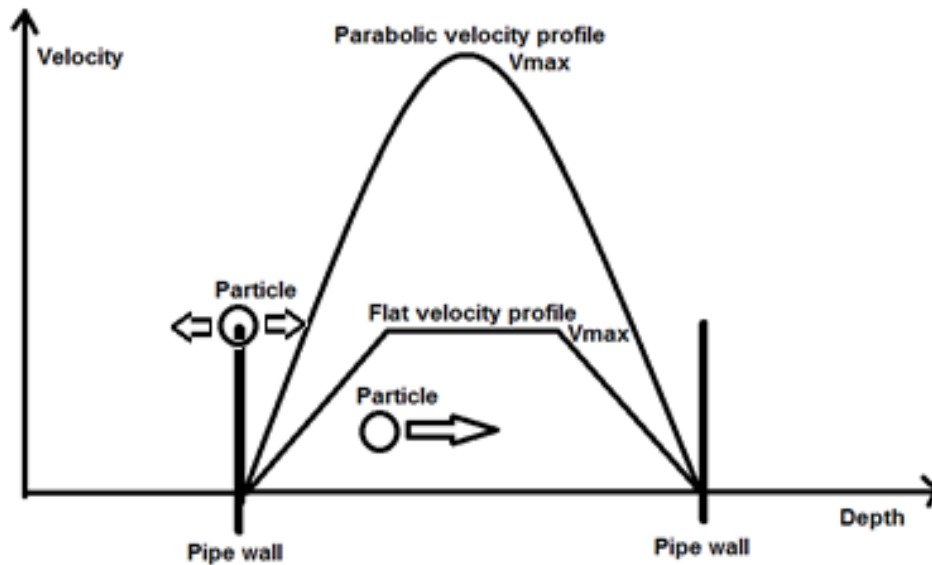


Figure 34 Illustration of simulation, shape of possible velocity profiles and position of pipe wall. The wall has to be simulated by a second particle.

There are several parameters that have to be set before the simulation can run:

1. The maximal velocity of the particle
2. The ultrasound basic frequency – is chosen to be similar to the ultrasound basic frequency in the measurements (2 MHz)
3. The speed of sound – same as in soft body tissue, because the original simulation should simulate the situation in the body (1540 m/s)
4. The number of steps the velocity should increase from the minimal to the maximal and then back to the minimal velocity – determines the smoothness of the profile
5. Pulse repetition frequency
6. Maximal travel distance. From the pulse repetition frequency (PRF) one can calculate the maximal distance the pulse can travel in the tube. The pulse must have time to return to the transducer before the next pulse is emitted. The actual width the particle shall travel is chosen to be a 10th of the maximal possible one.
7. The sampling frequency which determines the number of gates.

The parabolic velocity profile is created by a quadratic function with the preset maximal velocity at its maximum. Zero velocity has to be excluded otherwise the particle will never move forward. The flat profile is separated in three parts that have the same length: the increasing velocity part, the part with constant maximum velocity and the decreasing velocity part.

The particle starts at minimum velocity and proceeds through the pipe. It is recorded at every gate. The velocity of the particle changes according to the velocity profile. The emitted pulse is simulated as sinusoidal of five cycles with 2 MHz frequency. The pulse is filtered with a hamming filter which modulates the amplitude of the pulse. The received signal (RF-signal) is created by filtering the object function with the emitted pulse (Figure 35 b)). The object function has the length of the depth axis. All entries except at the actual position of the particle and the wall are zero. From the filtered object function the discrete-time analytic signal ( $X = X_r + iX_i$ .  $X_r$ : original pulse;  $X_i$ : Hilbert transform of pulse) is computed (Figure 35, c)). This step is done in order to obtain only positive frequencies later in the spectrum. The final signal is obtained after down mixing the analytic signal by weighting it with  $\exp(-2\pi f_0 t)$ ; where  $f_0$ : ultrasound frequency,  $t$ : time. The output I/Q data created in this way is used for testing the image based velocity estimation algorithm (Figure 35 d)).

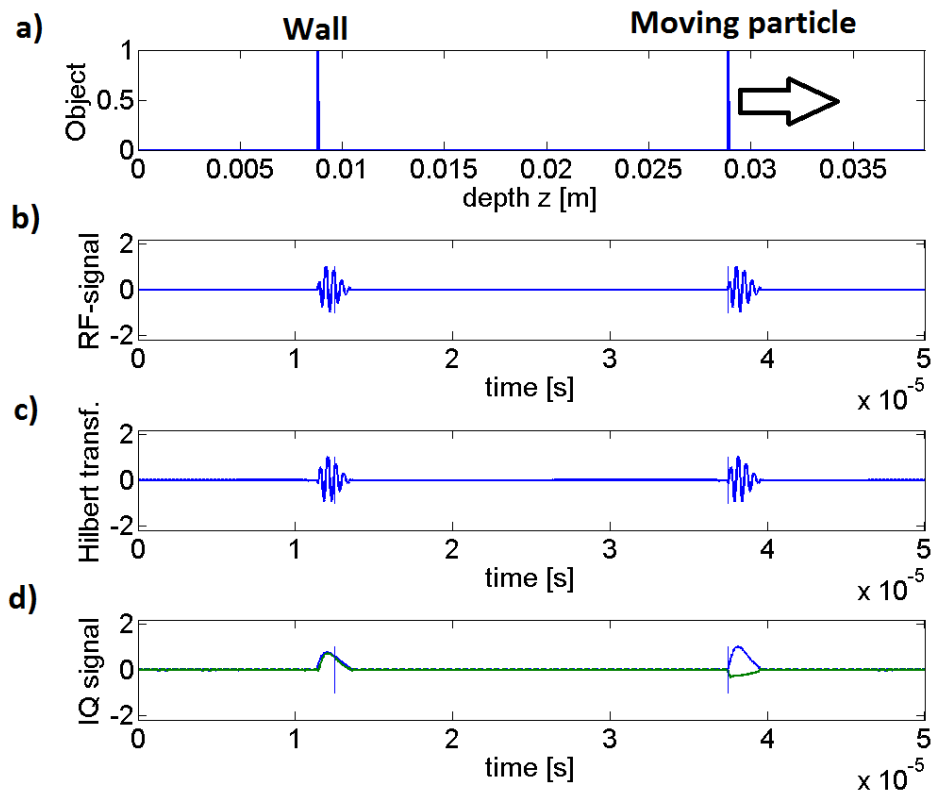


**Figure 35** Signal of simulation of one particle moving across the pipe diameter. b) RF-signal. c) Imaginary part of Hilbert transformation of RF-signal. d) I and Q signal are the real and imaginary part of the Hilbert transform after down mixing.

## 6.1.2 Results from test on simulation

The following settings were tested:

1. No optional profile detection functions
2. Averaging of image (filter size 25 x 25)
3. Averaging + Both edges (BE)
4. Averaging + Both edges(BE) + Prevent increase of velocity (PIOV)

The simulation has been run with a pulse repetition frequency of 4000 Hz and the maximal velocity of the particle of 0.8 m/s. No averaging over several profile blocks is needed because there is no statistical fluctuation between profile blocks originating from the simulation.

The results are shown and compared in *Figure 36* and *Figure 37*. The image profile without averaging is very noisy. The velocity profile is too narrow and not very accurate. That is because one of the noisy peaks at the center of the pipe is used for rescaling. It is necessary to apply an averaging filter to smooth the image. The image profile is highly improved after that but the sides of the image profile have no really good overlap with the real velocity. The FFT-profile has a better overlap.

This problem can be overcome by detecting both profile edges and use the average for the velocity estimation. The overlap with the real velocity profile at the sides is very good (*Figure 37a*). Prevention of increase of velocity at the wall (PIOV) removes the spike in the image profile at the wall. Instead the velocity is interpolated to the detected wall.

The detected wall gate does not agree with the real wall position. The velocity profile is cut off too early. The reason for that is the overlap of the wall echo with the particle's echo which is due to the implementation of the simulation and therefore it cannot be said that the wall position is falsely determined in general.

Nevertheless, it is possible to compare the effect of the averaging filter on the wall gate position. The averaging filter does not affect the detected wall gate position (wall gate coordinate without averaging: 359; with averaging: 354. Difference of 5 gates = 0.15 mm with a total gate number of 1200 = 38 mm is negligible).

The same observations were made for the flat velocity profile. As can be seen in *Figure 38* leads the application of an image averaging filter to a smoothing of the profile. Using both edges compensates distortions of the single edges and increases the accuracy and the peak of the image profile at the wall is removed by PIOV.

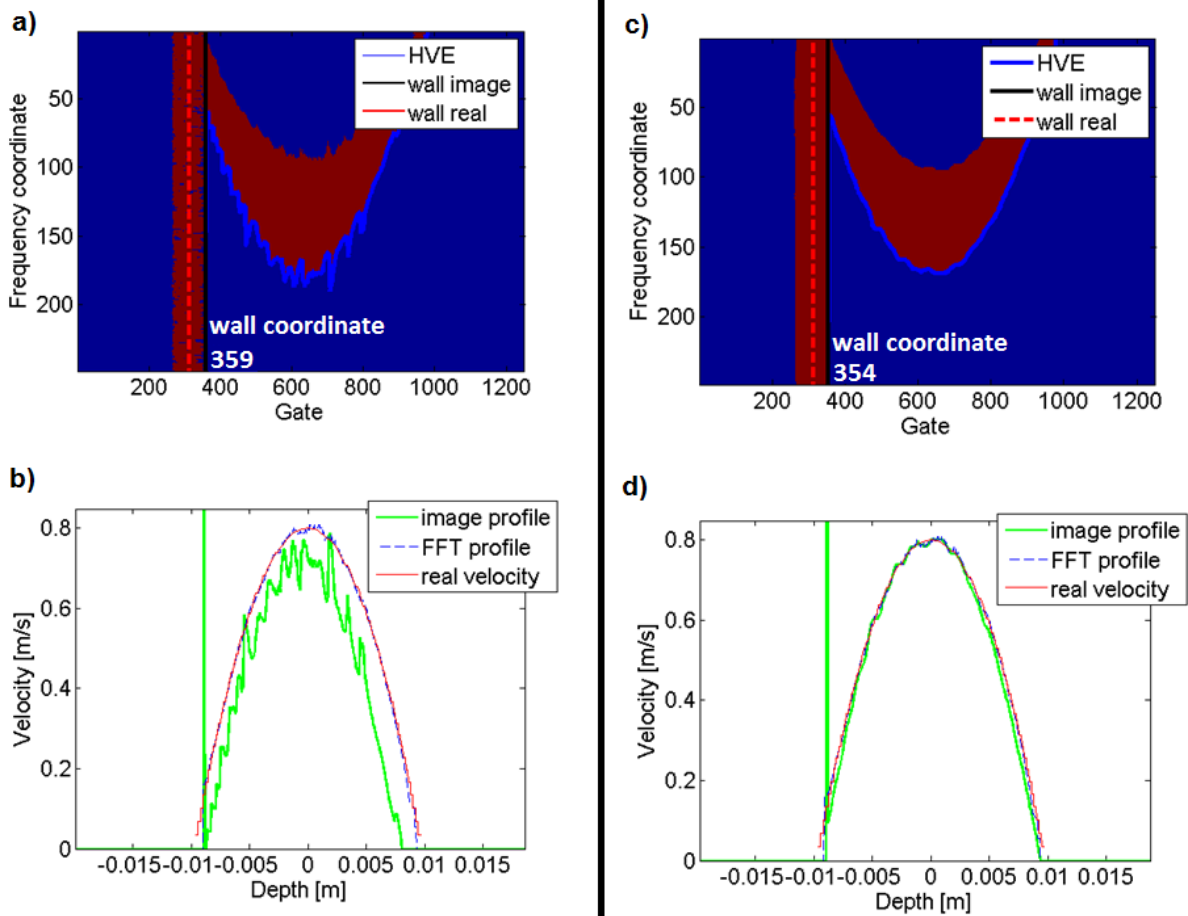


**Figure 36** a) Binary image of simulated parabolic velocity profile. No optional functions were applied. b) Comparison of different velocity profiles. Without any applied optional functions the image profile is very noisy. The FFT-profile overlaps pretty well with the real profile. c) Binary image after application of averaging filter. The edge a lot smoother compared to a). d) Because of the smoothing the image profile is less noisy. At maximal amplitude the overlap with the real velocity is pretty good, but at the sides the image profile is narrower than the real velocity profile.

## Evaluation of image based velocity estimator

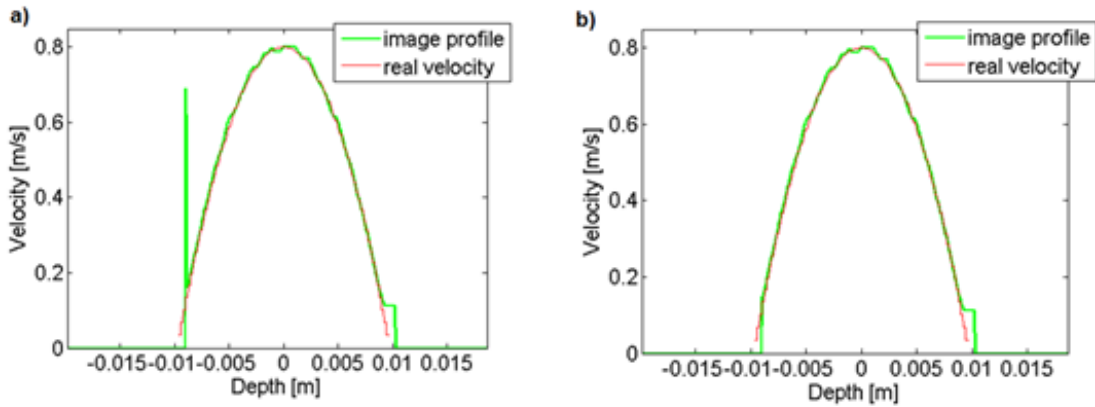


**Figure 37** a) Velocity profile after averaging of image and usage of both edges. b) Velocity profile after averaging of image, usage of both edges (BE) and prevention of increase of velocity at the wall (PIOV). In both cases the profile overlaps very well with the real velocity. Even at the sides. The usage of both edges improved the accuracy.

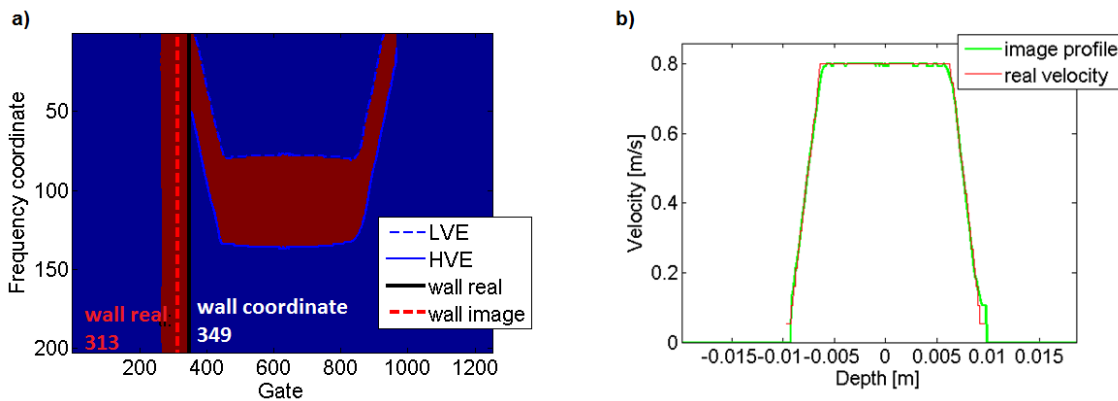


**Figure 38** a) Binary image of simulated flat velocity profile. The profile edges were detected. At the plateau the edges are curved. b) Comparison of image profile and real velocity profile. The curvature at the plateau is nearly compensated by using the average of both edges.

---

## 6.2 Test of code on real measurement data

The performance of the code and the optional function are tested on real measurement data from oil, ketchup and grout. Oil is a Newtonian fluid and has a parabolic velocity profile while ketchup is a Herschel-Bulkley fluid and exhibits plug flow.

Grout can be described as Bingham fluid; its rheology is dependent on the water/cement ratio, type of cement, additives, temperature (Wiklund J. a., 2012).

In grout it is difficult to reach a high penetration depth because of high particle concentration. The pipe diameters for oil and ketchup were 48.4 mm and for grout 22.6 mm.

The following aspects were tested for their effect onto wall detection, velocity profile's shape and processing time:

1. Variation of the threshold ratios for the generation of the binary image
2. Variation of number of pulse repetition
3. Variation of number of profile blocks
4. Functions for profile detection (BE,PIOV,CS)

### 6.2.1 Variation of threshold ratio

For the investigation of the influence of variation of the threshold ratio the average over four profile blocks with 512 pulse repetitions each was used to calculate the Doppler spectrum of oil.

The binary image is generated after the application of the threshold intensity value.

The threshold intensity value should be set in a way so that the profile is continuous and smooth and the outer edge can be detected. The detected wall position has to be reasonable. That means the detected wall position should agree with the wall position that is seen in the image of the Doppler spectrum. If only 0.6% of the pixels are erased the detected wall gate coordinate is not appropriate as can be seen in *Figure 40*. Too many pixel values are kept and hence the threshold intensity value is too low and the wall edge is detected too far from the clearly visible wall edge. If too many pixels are erased (0.8%) the profile is not continuous and too narrow (*Figure 39*). The outer edge of the profile cannot be detected.

The automatic threshold and erasing 0.7% of the pixels give reasonable profile shapes and wall positions as can be seen in *Figure 39* and *Figure 40*.

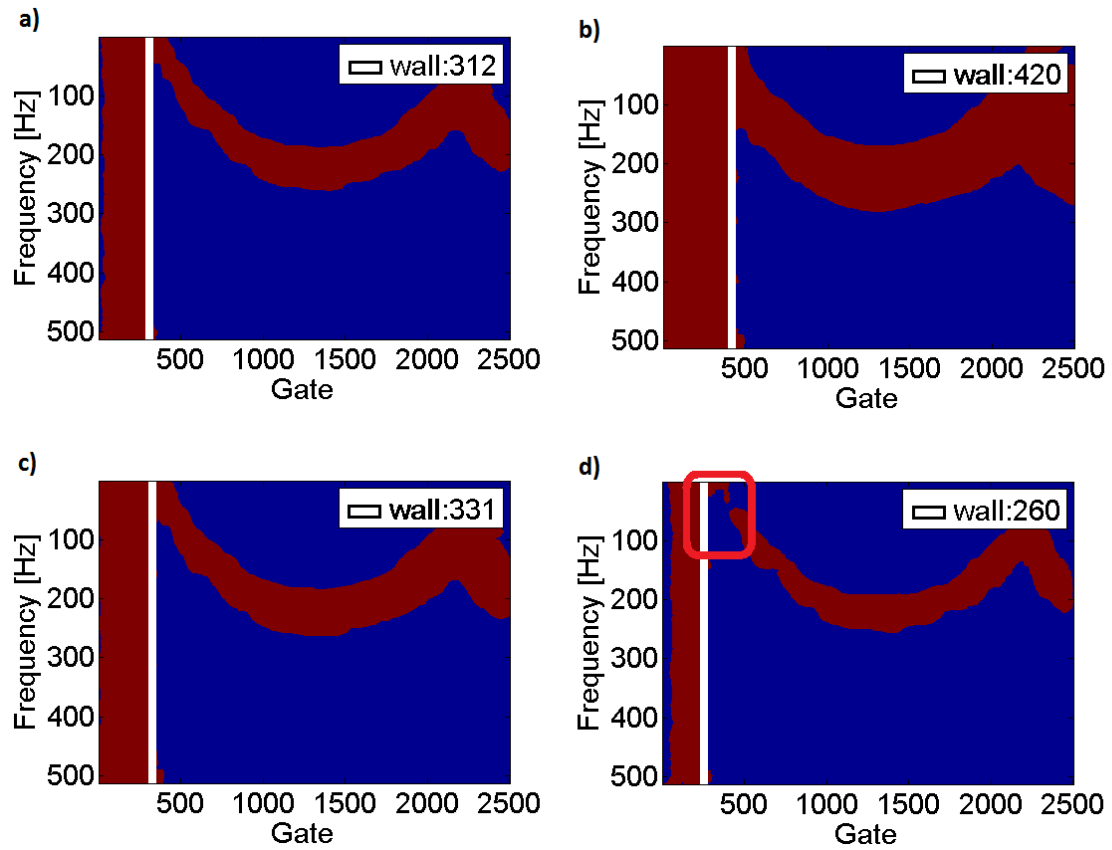


**Figure 39** Binary images of measurement with oil using 512 pulse repetitions and 4 profile blocks after application of a) automatic threshold. The profile is continuous and the wall position reasonable. b) Ratio 0.6. Too few pixels are erased. The profile is broad and smooth but the wall position has a too great depth. c) Ratio 0.7. The flow profile is continuous and the wall position reasonable. d) Ratio 0.8. Too many pixels are erased. The profile is not continuous anymore.

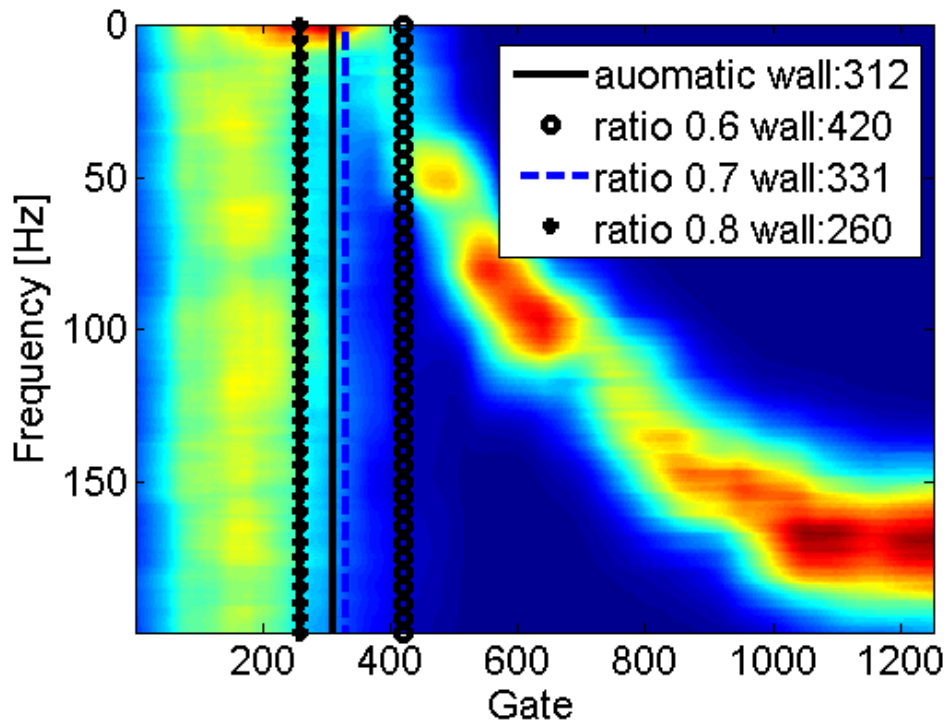


*Figure 40* Detected wall positions after application of different threshold intensity values. Measurement originates from oil with 512 repetitions and 4 profile blocks. The automatic ratio and a ratio of 0.7 agree well with the wall in the image of the Doppler spectrum.

## 6.2.2 Variation of number of number of pulse repetitions and profile blocks

The variation of pulse repetitions per profile block and the number of profile blocks determine the processing time. It is preferable to use as little pulse repetitions and profile blocks as possible to reduce the computing time. At the same time it is required that the profile shape and wall position are accurate. The effect of the variation of both, the number of pulse repetitions and number of profile blocks onto the wall position, profile shape and processing time is summarized in *Tables 1-2* and can be visually compared with the help of *Figures 41-44*.

For all profiles the functions BE, PIOV and CS for profile detection were used.

### 6.2.2.1 Variation of number of pulse repetitions

In order to compare the effect of variation of number of pulse repetitions only one profile blocks was used for computing the Doppler spectra of oil.

Oil data was chosen because it is known that behaves like a Newtonian fluid and the velocity at the wall has to be zero.

Decreasing the number of pulse repetitions reduces the image quality as it becomes evident comparing *Figure 41* and *Figure 42*.

The Doppler spectrum is more noise if only 64 pulse repetitions (PR) are chosen compared to the Doppler spectrum if 512 pulse repetitions are used.

The wall is successfully detected according to the image.

However, because of the poor image quality the detected wall coordinate is shifted to greater depth. Hence, it is not possible to detect the whole profile edge. It is cut off so that the velocity at the wall is not zero.

The processing time is not significantly affected by changing the number of pulse repetitions (*Table 1*).

*Table 1 Comparison wall gate and processing times for variation of number of pulse repetitions<sup>6</sup>.*

Number of pulse repetitions	512	256	128	64
Wall gate	363	357	515	575
Depth [mm]	11.1	10.9	15.8	17.6
Time [s]	1.9	2.4	2.3	2.3

<sup>6</sup> The processing times that are given in the table are only comparable to each other, because the times depend on the data processor that was used for computations.

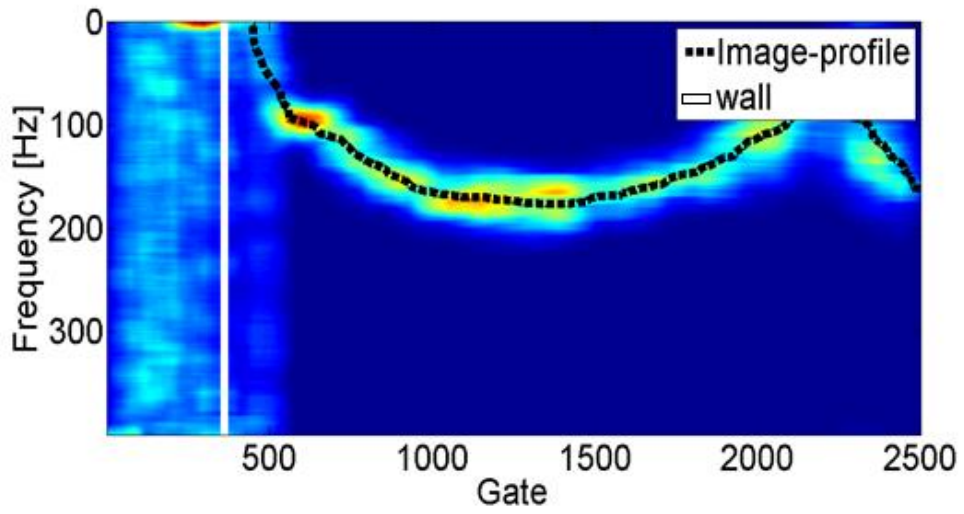


*Figure 41* Doppler spectrum of oil using one profile block with 64 pulse repetitions. The profile is distorted and the wall is not clear. The wall position is detected according to the wall that is visible in the image.

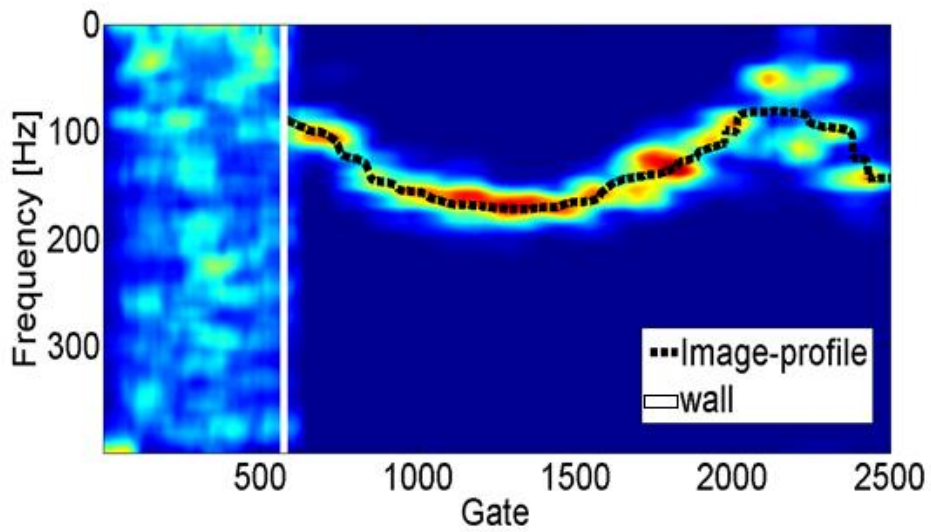


*Figure 42* Doppler spectrum of oil using one profile block with 512 pulse repetitions. The profile is fairly smooth but the wall is not clear. The wall position is detected according to the wall that is visible in the image.

The processing step of the image based velocity profile estimator that contributes the most to the total processing time is the interpolation step (Table 4).

The image is interpolated to 512 pixels in the vertical direction. If at least 512 pulse repetitions is used this step can be skipped. That is why the processing time using 512 pulse repetitions is even slightly less than for 128 and 64 pulse repetitions.

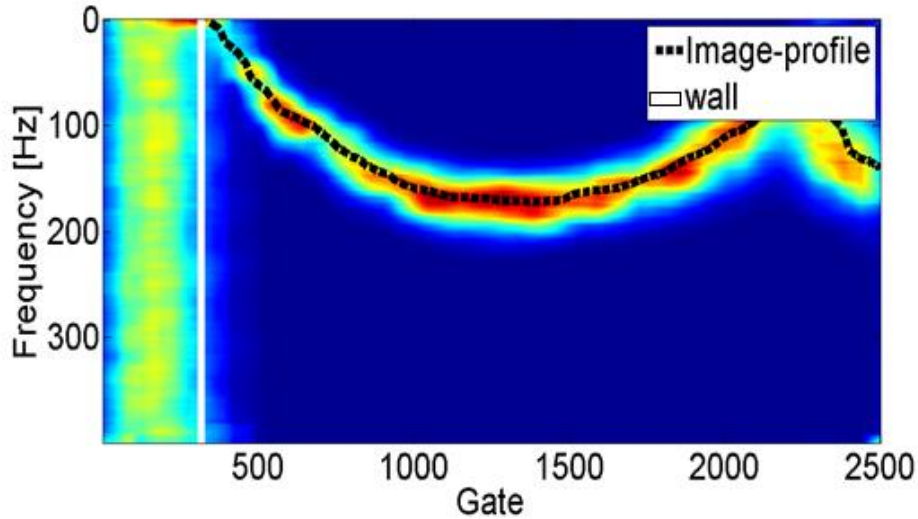


Figure 43 Doppler spectrum of oil using 4 profile blocks with 512 pulse repetitions. The profile and the wall are clearly visible. The wall position is detected according to the wall that is visible in the image.

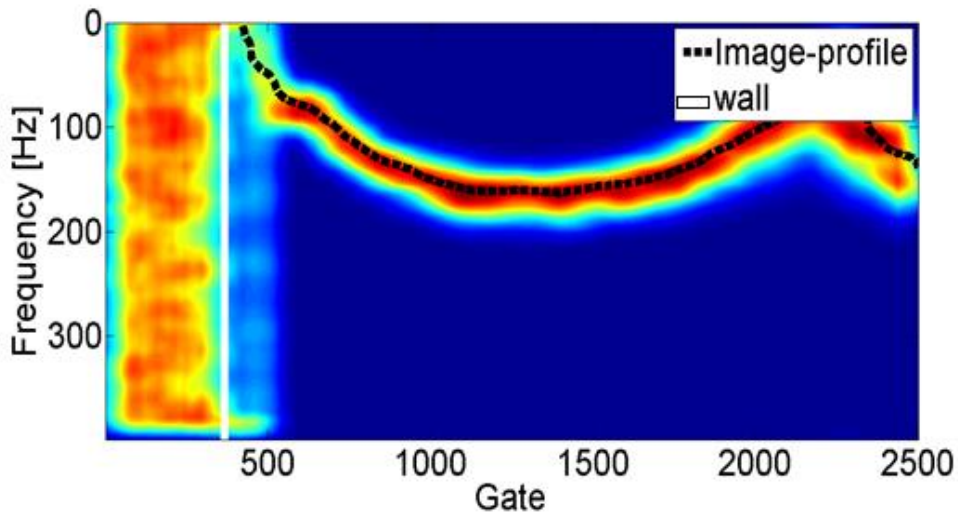


Figure 44 Doppler spectrum of oil using 32 profile block with 64 pulse repetitions. The profile and the wall are clearly visible. The wall position is detected according to the wall that is visible in the image.

## 6.2.2.2 Variation of number of profile blocks

Profile blocks do not look identical because of statistical variations between the pulses. The particles do not move all in the same manner and the flow rate can fluctuate slightly. Therefore it can be necessary to use several profile blocks and compute the average in order to get a more accurate results for the velocity profile.

Comparing the Doppler spectra for 512 pulse repetitions using one (*Figure 41*) or four profile blocks (*Figure 43*) it is evident that averaging over more profile blocks results in a clearer image. The profile is not as strongly distorted and the wall edge is more prominent than when only one profile block is used.

If only one profile block is used the wall is detected according to the image as can be seen in *Figure 41*. It is detected at a greater depth because the wall in the image is blurrier. Zero velocity is approached several gates before the wall.

A similar effect is seen if one profile block with 128 or 64 pulse repetitions was used. If too few profile blocks are taken into account the wall is blurry. It is necessary to use even more profile blocks to get an equally accurate result if less pulse repetitions are chosen. One profile blocks with only 64 pulse repetitions lead to an unclear profile (*Figure 42*). If 32 profile blocks (*Figure 44*) are used the wall and the profile becomes equally clear as if four profile blocks with 512 pulse repetitions are used,

*Table 2 Comparison wall gate and processing times for variation of profile blocks with 512 pulse repetitions<sup>7</sup>.*

Number of profile blocks	1	2	4
Wall gate	363	315	319
Depth [mm]	11.1	9.6	9.8
Time [s]	1.9	2.6	3.6

*Table 3 Comparison wall gate and processing times for variation of profile blocks with 128 pulse repetitions<sup>7</sup>.*

Number of profile blocks	1	16	32
Wall gate	575	493	367
Depth [mm]	17.6	15.1	11.2
Time [s]	2.4	8.68	15.4

<sup>7</sup>The processing times that are given in the table are only comparable to each other, because the times depend on the data processor that was used for computations.

## Evaluation of image based velocity estimator

---

**Table 4** Time contribution of the most time consuming processing parts of the velocity estimator.

Function	Time [s]
interpolation	Ca. 0.8
Get wall	Ca. 0.3

The drawback of using more profile blocks is a longer processing time. If 32 profile blocks are used instead of only one the processing takes almost five times as long (*Table 3*). The processing time is increased because for every profile block the Doppler spectrum has to be computed which is time consuming.

The displayed cases of oil (*Figure 41-42*) suggest that it is better to use a higher number of pulse repetitions and to average over only a few profile blocks.

The actual number of pulse repetitions and profile blocks that should be used for different fluids is dependent on the fluid and the image quality. It has to be tested which parameters give the most accurate results.

## 6.2.3 Validation of profile detection functions

For the validation of the profile detection functions (HVE, BE, PIOV) four profile blocks with 512 pulse repetitions were used. The automatic threshold intensity value was applied for the generation of the binary image.

### 6.2.3.1 Oil

In *Figure 45* velocity profiles of oil originating from HVE, BE are compared with the FFT-velocity profile. The velocity profiles obtained from HVE and BE are smoother than the FFT-velocity profile. That is because the image was smoothed with an image averaging filter. The most prominent artifact of the image based velocity estimator is the wall edge that is falsely assigned as part of the profile (*Figure 45*, (1)). Apart from that do the HVE and BE velocity profiles fluctuate less close to the wall than the FFT-profile. The FFT-velocity profile does flatten out stronger. The BE velocity profile is less rugged compared to the HVE velocity profile (*Figure 45*, (2)) and overlaps with the FFT-profile at the far side of the pipe (*Figure 45*, (3)).

The problem with falsely assigned wall edges can be taken care of by preventing the increase of velocity with the custom PIOV function.

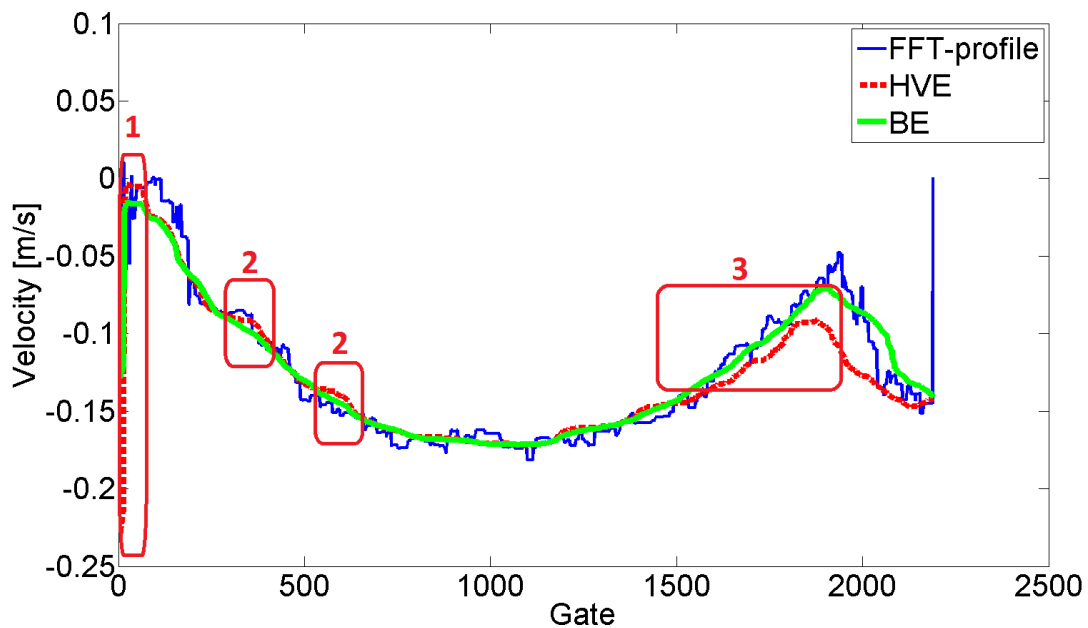


*Figure 45* Measurement with oil. Comparison of FFT-velocity profile with HVE- and BE-velocity profiles. The image based velocity profiles (HVE and BE) are smoother. (1) Artifact of image based profile extraction. Wall edge is falsely assigned as part of the profile. (2) BE is less rugged than HVE. (3) BE overlaps with FFT-velocity profile.

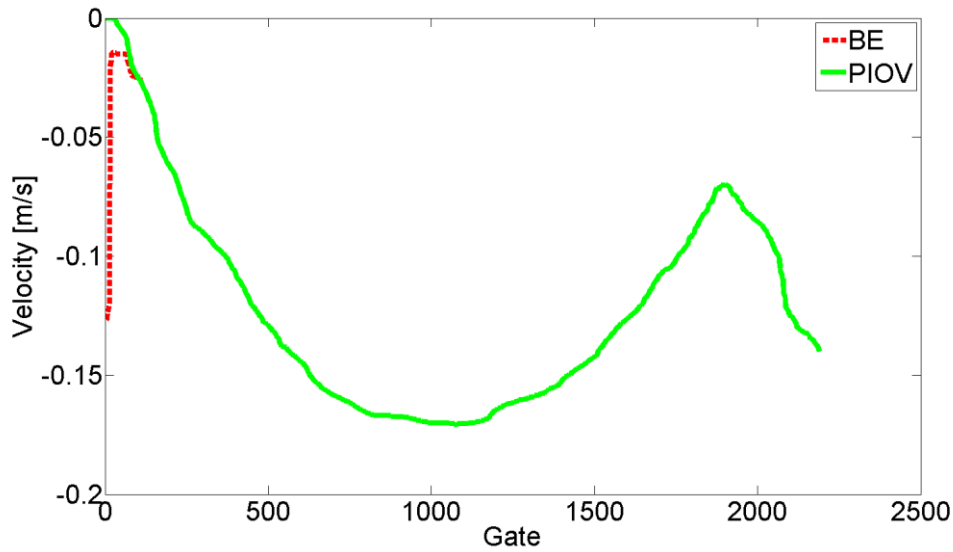


Figure 46 Measurement with oil. Comparison of BE velocity profile and after application of PIOV onto BE. Falsely assigned wall edges are corrected by application of PIOV. The velocity continues to decrease at the edge.

After application of PIOV the velocity profile does continue decreasing to the wall (Figure 46). However, the PIOV velocity profile does reach zero velocity a few gates before it reaches the wall gate.

It could be argued that a faster way to obtain a smooth profile would be to apply an averaging filter onto the FFT-profile.

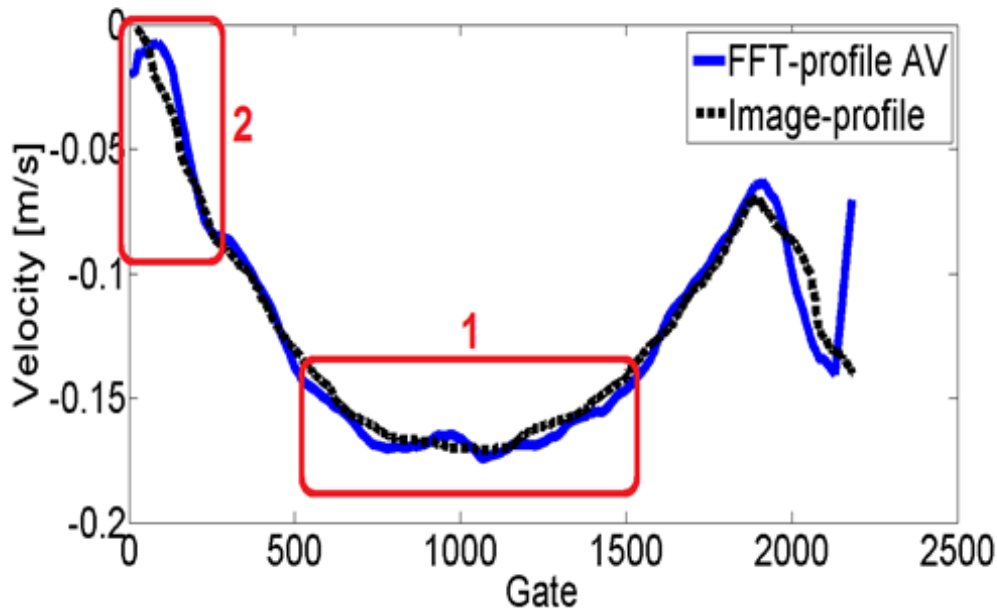


Figure 47 Comparison of averaged FFT-profile and image profile. Although the FFT-profile is smoothed it is more rugged than the image-profile (1). The FFT-profiles velocity increases at the wall (2).

This was done and the averaged FFT-profile (FFT-profile AV) and the image-profile are compared in *Figure 47*. As can be seen in *Region 1* of *Figure 47* the Image-profile is still smoother than the FFT-profile. At the wall the velocity of the averaged FFT-profile increases while the image-profiles continue to decrease.

### 6.2.3.2 Ketchup

After the test of the image based velocity estimator functions on the measurement of oil and the test on the simulation (*Section 6.1*) it seems reasonable to use BE and PIOV. However, if the estimates of HVE+PIOV and BE+PIOV are compared for a measurement of ketchup (*Figure 48* and *Figure 49*) the conditions are different.

The velocity is not zero at the wall because of wall-slip. The velocities at the wall differ quite a lot between HVE+PIOV with 0.01 m/s and BE+PIOV with 0.02 m/s.

The shape of the BE+PIOV-velocity profile is less rugged than the HVE-PIOV profile as can be seen in *Region 2*, *Figure 48* and it has no kink close to the wall as in *Region 1*, *Figure 48*. The kink originates from the distortion of the profile that is caused by convolution of the velocity profile with the sampling volume. It is important to detect a velocity profile without the kink hence just by looking at the shape of the velocity profile BE+PIOV is the better choice for velocity profile estimation.

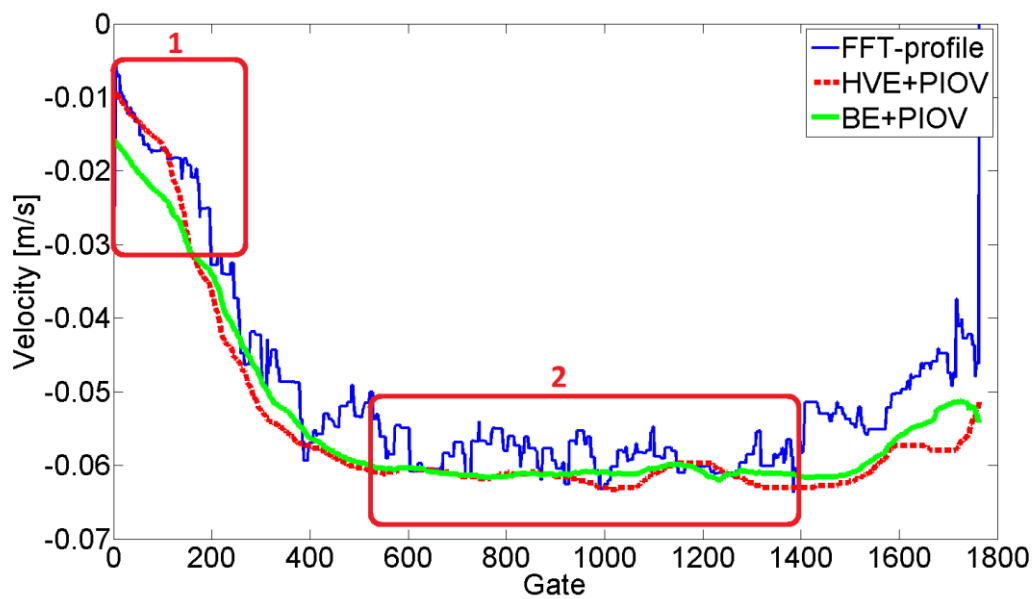


*Figure 48* Comparison of velocity profiles of ketchup. HVE+PIOV has the problem of flattening at the wall. BE+HVE exhibits no flattening but the velocity at the wall could be too high (1). Both image based profiles are smoother than the FFT-profile (2). BE+PIOV is smoother in the region of plug flow (2).

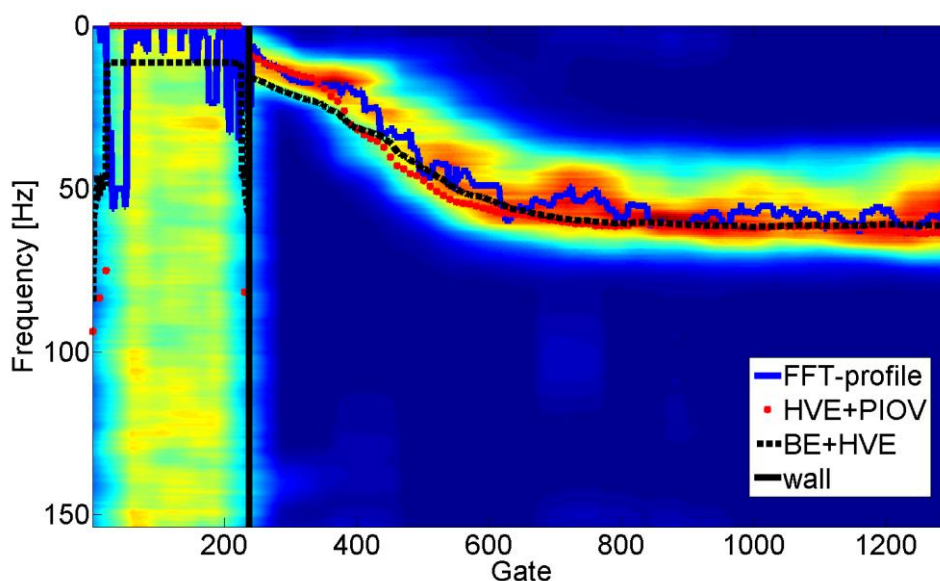


*Figure 49 Doppler spectrum ketchup. The wall agrees well with the edge in the image. HVE+PIOV has the problem of flattening at the wall. BE+HVE exhibits no flattening but the velocity at the wall could be too high.*

The velocity that HVE+PIOV estimates at the wall is closer to the value that the FFT method predicts. The rheology that is estimated from the HVE+PIOV and BE+PIOV profile has to be compared with the rheology that is measured with off-line rheometers. In this way it is possible to decide which result is more accurate. In *Section 6.2.4* the image based velocity estimator performance concerning the determination of the correct rheology is compared with the FFT-method and the result from off-line rheometry.

In *Figure 50* and *Figure 51* the shape of velocity profiles that were obtained from Doppler spectra using either one profile block with 64 pulse repetitions or the average over 32 profile blocks with 64 pulse repetitions are compared in order to show that especially for low pulse repetition numbers the performance of the image based velocity profile estimator is superior to the FFT method. For only one profile block the FFT-profile is very noisy and it is impossible to determine the correct rheology from a velocity profile that has a shape like that (*Figure 50*). Compared with the FFT-profile is the HVE+PIOV profile much smoother. Especially close to the wall is the velocity gradient smooth and realistic. If 32 profile blocks are used for averaging the FFT-profile is smoother but still more rugged than HVE+PIOV (*Figure 51*). The processing time for 32 profile blocks is with 10.23 seconds almost double as long as for using only one profile block with 5.53 seconds. That shows that the image based approach is clearly superior to the FFT method because it gives fairly good results even for a low number of profile blocks. In this way the processing time can be reduced.

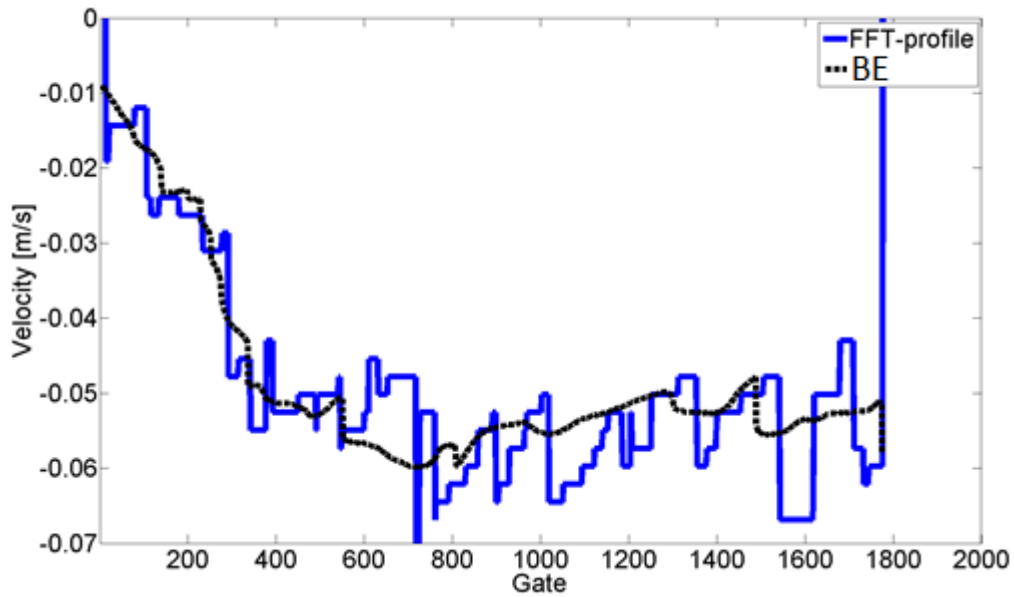


**Figure 50** Comparison of FFT-profile and BE image profile using one profile block with 64 pulse repetitions. The image based velocity profile is a lot smoother than the FFT profile and has a realistic velocity gradient at the wall. The processing time is 5.53 seconds<sup>8</sup>.

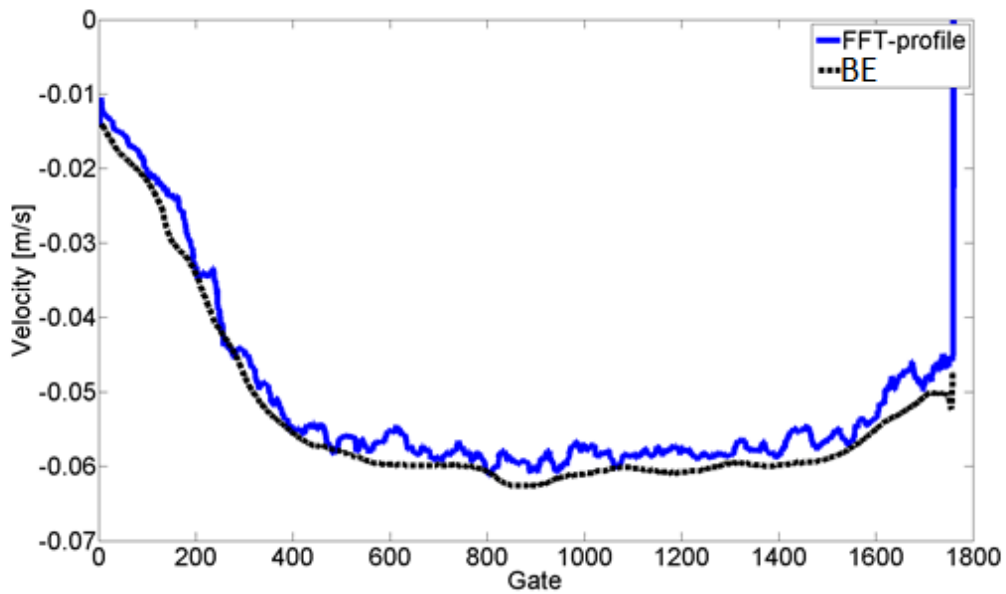


**Figure 51** Comparison of FFT-profile and BE image profile averaging over 32 profile blocks with 64 pulse repetitions. It takes double as long to process 32 profile blocks than to process only one profile block with 64 pulse repetitions. Still is the image based velocity profile smoother than the FFT profile. The processing time is 10.23 seconds<sup>9</sup>.

<sup>8</sup> The processing times that are given in the table are only comparable to each other, because the times depend on the data processor that was used for computations.

### 6.2.3.3 Grout

In grout it is difficult to reach a high penetration depth because of high particle concentration. This is significantly noticeable when looking at the Doppler spectrum of grout. Even though the diameter of the pipe is only 22.6 mm instead of 48.4 mm as in the case of ketchup and oil it is not possible to determine the velocity profile anymore in *Region 1* in *Figure 52*. The signal to noise ratio is too low.

Comparing the velocity profiles HVE+PIOV and BE+PIOV (*Figure 53*) shows that BE-PIOV is less rugged at low depths and it does not reach zero velocity before the wall. However, at a greater depth BE-PIOV is affected by the high noise level and the step that is visible in *Figure 52*, *Region 2*. That is because the lower velocity edge cannot be estimated in that region and the average of both edges distorts the velocity profile in that case.

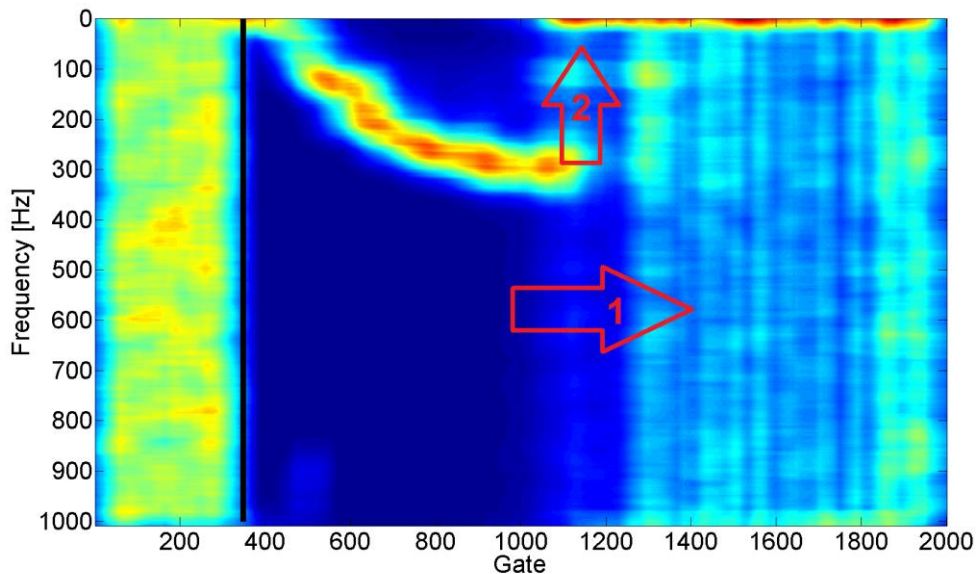


*Figure 52* 1: Doppler spectrum grout. High attenuation reduces the penetration depth at (1) it is not possible to detect a profile. If BE is used the step at (2) causes distortion of the image-profile. Wall position agrees well with wall edge in the image.

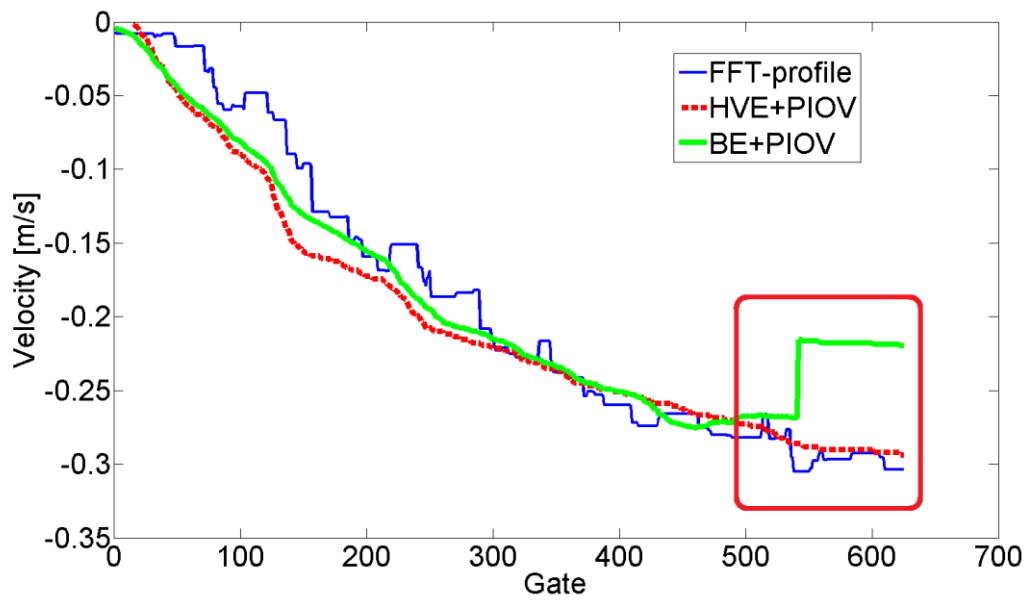


*Figure 53 Comparison of velocity profiles from grout. HVE+PIOV does reach zero velocity a few gates before the wall gate is reached. BE+PIOV gives a nice profile shape but at great depths the high level of noise in the Doppler spectrum distorts the lower velocity edge and thus BE.*

## 6.2.4 Rheology of ketchup

Eventually, the rheology of ketchup that was estimated by the old FFT based method and the new image based method was compared with rheological data that had been measured with an off-line rheometer.

The image was generated using one profile block, but different numbers of pulse repetitions were tested. Instead of averaging over several profile blocks another kind of averaging was applied. The signal of all pulse repetitions at every gate was divided into half. Then FFT with the FFT length of the original number of repetition was applied and eventually the average of the two parts was calculated. The images that are generated when this method of averaging is applied are similar to the images that are generated by the method of averaging profile blocks. The difference is that processing times increase if a higher number of pulse repetitions is used. It was possible to find the correct rheology with both methods.

The FFT-profile gives the correct rheology if the wall position was manually preset to the calculated wall position at gate 380 and 2048 pulse repetitions were used (*Figure 54*). In this case the preset wall position does not agree with the wall edge that is visible in the image of the Doppler spectrum. The high number of pulse repetitions is needed in order to obtain a smooth FFT-profile and to be able to derive the correct rheology from it.

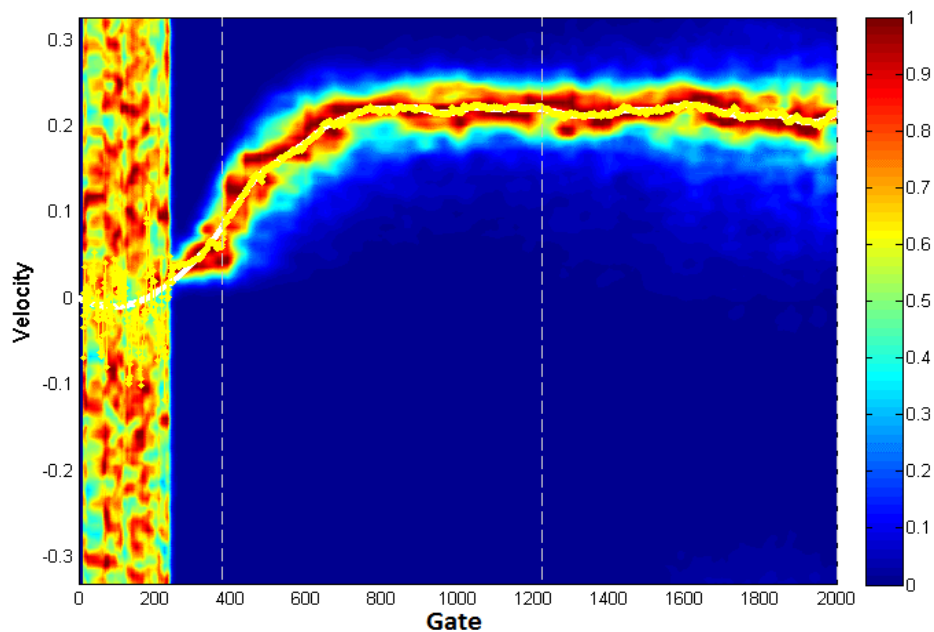


*Figure 54* Doppler spectra of ketchup using 2048 pulse repetitions with FFT-profile (yellow, dotted-line) and Image-profile (white solid line). The wall position at gate 380 was The vertical dotted lines mark the wall positions at both sides of the pipe and the pipe center.

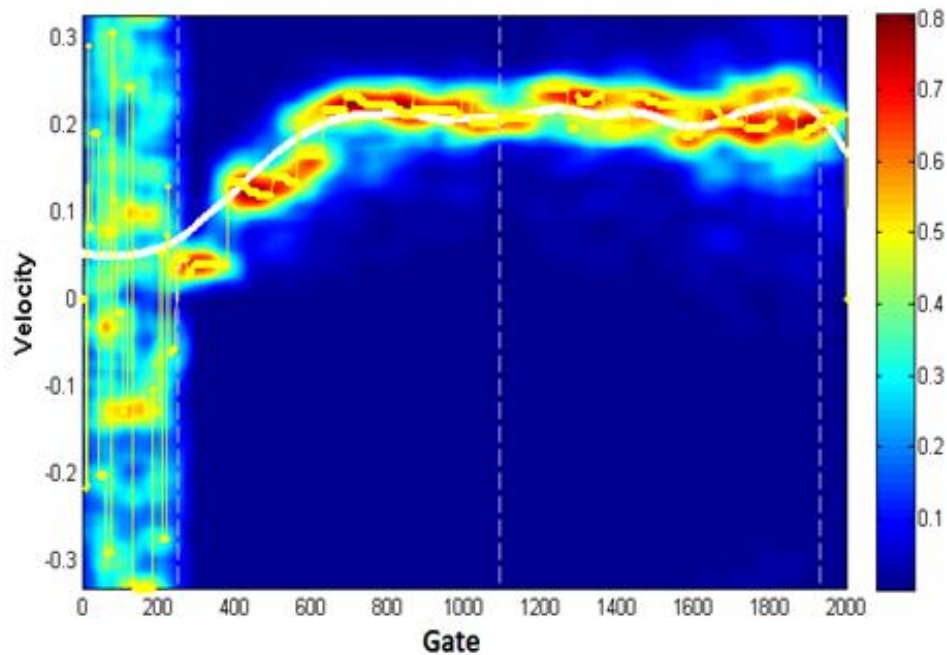


*Figure 55* Doppler spectra of ketchup using one 128 pulse repetitions with FFT-profile (yellow, dotted-line) and Image-profile (white solid line). The wall position at gate 249 was estimated by means of image analysis. The image-profile is a lot smoother than the FFT-profile. The vertical dotted lines mark the wall positions at both sides of the pipe and the pipe center.

The image based method detected the wall that is visible in the image at gate 249. For the image-profile wall position at gate 249 and only 128 pulse repetitions give the correct rheology (*Figure 55*). The image-profile was extracted rescaling the higher velocity edge (HVE) and prevent increase of velocity (PIOV). Comparing the FFT-profile with the image-profile using only 128 pulse repetitions it is obvious that the image-profile has the better shape. It is very smooth while the FFT-profile is very noisy. It was tested whether the combination of the wall that is detected by means of image analysis at gate 249 and the FFT-profile can give the correct rheology. That was neither the case if 128 pulse or 2048 pulse repetitions were chosen. Even though the FFT-profile is very smooth for 2048 pulse repetitions it has an unrealistic velocity gradient close to wall gate 249. The FFT-profile suffers under distortion because of the convolution of velocity profile and sampling volume. The flow curves that can be derived from the image-profile and the FFT-profile in combination with pressure difference measurements are displayed in *Figure 56*.

The processing time is reduced from 11.63 seconds for the FFT method using 2048 pulse repetitions to 5.59 seconds using 128 pulse repetitions for the image based method.

Due to changes of temperature, vibration of the pipe or changing the pulse length it is important to be able to detect the wall automatically. It is not possible to preset the wall position manually for industrial monitoring.

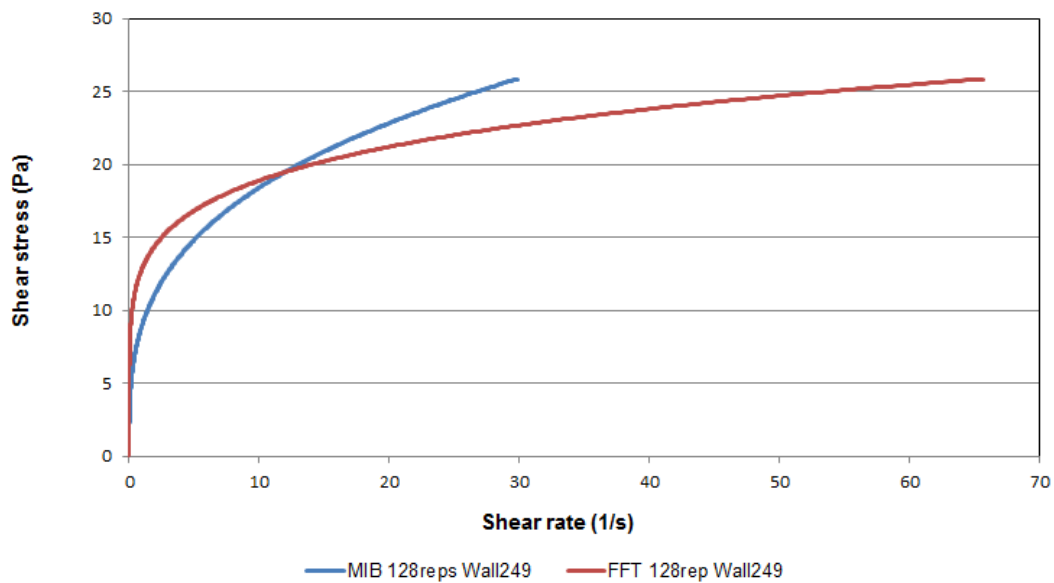


**Figure 56** Flow curves of ketchup obtained with the image based velocity profile estimator and FFT-profile. The image based velocity profile (MIB) using 128 pulse repetitions and wall 249 results in the correct rheological result while the FFT-profile under the same conditions leads to a wrong rheological estimate.

Therefore it is a clear improvement to be able to detect the wall automatically with the image based method for each profile and to estimate a realistic velocity profile and especially a realistic velocity gradient at the wall that gives the correct rheology in half the time.



# 7 Conclusion and outlook

## 7.1 Conclusion

In this work an image based velocity profile estimator was developed. With the aid of a simulation it was shown that the new velocity estimator has the potential to estimate the correct velocity profile if both profile edges are detected, rescaled and used for the estimation of the velocity profile. However, falsely assigned wall edge pixels have to be corrected by preventing the velocity to increase at the wall (PIOV) and possibly correct steps (CS).

The validation of the new velocity profile estimator shows that it can detect the edge that is visible in the Doppler spectrum using an automatic threshold. A high noise level might require adjusting the threshold ratio.

It is advisable not to use a too low number of pulse repetitions, because the wall position is shifted to too great depths otherwise. A higher number of pulse repetitions does not change the processing time of the imaged based velocity profile estimator.

Because of statistical fluctuations between profile blocks it is beneficial to use the average over a few profile blocks for further processing. The number of profile blocks used for averaging should be kept low because it increases the processing time. It is necessary to compromise between smooth profile shape and processing time. Generating the Doppler spectrum is the time limiting factor.

The wall that is visible in the image is detected successfully. From the detected wall coordinate the velocity profile is detected

Application of BE+PIOV result in the smoothest velocity profile and exhibit almost no flattening at the wall. HVE+PIOV exhibit quite often a slightly flattening.

Both options result in smoother velocity profiles than the FFT-profile and are less flattened at the wall which is an improvement compared to the old method.

If the Doppler spectrum is very noisy and the penetration depth of the ultrasound pulse is low the usage of both profile edges can be problematic and distort the spectrum at greater depths of the pipe as in the case of grout.

The main objective of this work was to find the wall position automatically and estimate the correct velocity profile from that point.

Comparing the performance of the old FFT-method and the new image based velocity profile estimator for a measurement of ketchup shows that the newly developed method can automatically detect the wall and give the correct rheology in half the time that the FFT-method needs because the number of pulse repetitions needed to get an accurate and realistic velocity profile could be reduced.

---

## 7.2 Outlook & Recommendations

It was shown that there is the potential to make velocity profile estimation faster by applying an image based approach.

However, there is more testing to be done on a broad variety of different fluids with different flow behavior and flow velocities. The obtained rheology has to be compared with results from off- line measurements to make sure that it is accurate.

The image based velocity profile estimator has to be developed further in order to make it more flexible for different measuring conditions like a high level of noise. The parameter setting and choice of profile detection functions should be automated in order to make the application of the velocity estimator user friendly.

It has to be tested whether BE+PIOV or HVE+PIOV is the better alternative for more different measurements by comparing the obtained rheology with off-line rheology measurements.

For oil HVE+PIOV and BE+PIOV have sometimes the problem that the velocity profile approaches zero velocity before the estimated wall position. In order to obtain really accurate results the wall detection should be further improved. The wall position could be adjusted after profile detection by shifting it to the position where the profile reaches zero velocity.

The rheology of more measurement data has to be compared to see whether the imaged based velocity estimator is accurate and reliable. The estimator needs to be further improved if the noise level is high.

The number of input parameters should be decreased by adjusting the parameters automatically if the case requires that. This would make the velocity estimator more users friendly.





# Bibliography

- Banfill, P. (2003, May). The rheology of fresh cement and concrete - A review. *International Cement Chemistry Congress*.
- Barber, W. a. (1985). A New Time Domain Technique for Velocity Measurements Using Doppler Ultrasound. *IEEE Transactions on Biomedical Engineering*.
- Barnes, H. a. (1993). *An Introduction to Rheology*. Elsevier.
- Chodorowski, A. a. (2014). *Image Analysis Course*. Chalmers University of Technology.
- Durst, F. a. (1976). *Principles and practice of laser-Doppler anemometry*. London: Academic Press.
- Eisenberg, R. a. (1992). *Radiology: an illustrated history*. ST LOUIS :MOSBY.
- Embree, P. a. (1990). Pulsed Doppler accuracy assessment due to frequency dependent attenuation and Rayleigh scattering error sources. *IEEE Transactions on Biomedical Engineering*, 37(3).
- Ensminger, D. a. (2009). *Ultrasonics: Data, Equations and Their Practical Uses*. CRC Press Taylor & Francis Group.
- Evans, D. a. (2000). *Doppler Ultrasound - Physics, Instrumentation and Signal Processing (Vol. 2)*. John Wiley and Sons, LTD.
- Flow-Viz. (2004). *Flow-Viz brochure*. SIK-The Swedish institute for food and biotechnology.
- Flow-Viz. (2014). *Flow-Viz - Fluid Visualization & Characterization System, brochure*. SIK - The Swedish institute for food and biotechnology, Cape Peninsula University of Technology.
- Fredrickson, A. (1964). *Principles and Applications of Rheology*. Englewood Cliffs: Prentice-Hall.
- Green, P. (1964). Spectral Broadening of Acoustic Reverberation in Doppler-Shift Fluid Flowmeters. *The Journal of the Acoustic Reverberation in Doppler-Shift Fluid Flowmeters*(36), 1383.
- Hackmann, W. (1984). *Seek & Strike: sonar, anti-submarine warfare, and the Royal Navy, 1914-54*. London: H.M.S.O.
- Hatzikiriakos, S. (2012, April). Wall slip of molten polymers. *Progres in Polymer Science*, 37(4), 624-643.
- Holdsworth, S. (1993). Rheological models used for the prediction of the flow properties of food products: a literature review. *Food and Bioproducts Processing : Transactions of the Institution of Chemical Engineers, Part C*, 71, 139-179.
- Holmbom, M. (2011). *Evaluation and optimization of velocity estimators for pulsed ultrasound Doppler based velocity profile measurements*. Uppsala Universitet.
- Huang, J. a. (2007). Imaging Artifacts of Medical Instruments in Ultrasound-Guided Interventions. *J Ultrasound Med*, 1303-1322.
- ISUD. (2014). *ISUD*. Retrieved from International Symposium on Ultrasonic Doppler Methods for Fluid Mechanics and Fluid Engineering: [www.isud-conference.org](http://www.isud-conference.org)
- Jensen, J. (1996). *Estimation of blood velocities using ultrasound*. Cambridge Univerity Press.
- Jensen, J. (2001). *Linear description of ultrasound imaging systems*. Notes of the International Summer School on Advanced Ultrasound Imaging - Technical University of Denmark.
- Jones, S. (1993). Fundamental Sources of Error and Spectral Broadening in Doppler Ultrasound Signals. *Crc Critical Reviews in Biomedical Engineering*(21), 399-483.
- Jorgensen, J. a. (1973). Physical characteristics and mathematical modelling of the Puled Ultrasonic flowmeter. *Med. Biol. Eng.*, 11(4), 404-421.
- Kasai, C. a. (1985). Real-time Two-Dimensional Blood Flow Imaging Using an Autocorrelation Technique. *IEEE Transactions on sonics and ultrasonics*.

- Klafter, J. and Sokolov, I.M. (2011). *First Steps in Random Walks. From Tool to Application*. Oxford University Press.
- Kotzé, R. a. (2010). *Measurement and analysis of flow behaviour in complex geometries using the Ultrasonic Velocity Profiling (UVP) technique*. ELSEVIER.
- Kotzé, R. a. (2013). Optimisation of Pulsed Ultrasonic Velocitmetry sytem and transducer technology for industrial applications. *Ultrasonics*, 53(2), 459-469.
- Madlener, K. a. (2009). Generalized reynolds number for non-newtonian fluids. *Progress in Propulsion Physics*(1), 237-250.
- MetFlow. (2002). *Draft Edition, UVP Monitor, Model UVP-DUO with Software Version, User's Guide*. Met-Flow,SA.
- Met-Flow. (2002). *User's Guide*. MET-FLOW, Lausanne - Switzerland.
- Mueller, M. a. (1997). New rheometric technique: the gradiant-ultrasound pulse Doppler method. *Applied Rheology*(7), 204.
- Munson, B. a. (2009). *Fundamentals of fluid mechanics*. John Wiley and sons.
- Rahman, M. a. (n.d.). *In-line rheological measurements of cement grouts: Effects of water/cement ratio and hydration*. KTH-Royal institute of technology, Stockholm.
- Rao, M. (2014). *Rheology of Fluid, Semisolid, and Solid Foods*. Springer.
- Ronningsen, H. (2012). Rheology of Petroleum Fluids. *ANNUAL TRANSACTIONS OF THE NORDIC RHEOLOGY SOCIETY*.
- Shutilov, V. (1988). *Fundamental physics of ultrasound*. Gordon and Breach Science Publishers.
- Steffe, P. F. (1996). *Rheological methods in food procesing engineering* (Vol. 2). Freeman Press.
- Takeda, Y. (1986). *Velocity profile measurement by ultrasound Doppler hift method*. ELSEVIER.
- Torp, H. (2004). *Estimation of blood velocities from Doppler signals*. ISB, NTNU.
- Tortoli, P. (1996). Spectral Velocity Profiles for Detailed Ultrasound Flow Analysis. *IEEE Transactions on Ultrasonics, Ferroelectrics, and Frequency Control*, 43(4), 654-659.
- Wiklund, J. (2007). *Ultrasound Doppler Based In-Line Rheometry - Development, Validation and Application*. Doctoral thesis at Lund University.
- Wiklund, J. a. (2007). Methodology for in-line rheology by ultrasound Doppler velocity profiling and pressure difference techniques. *Chemical Engineering Science*, 62(16), 4277-4293.
- Wiklund, J. a. (2012). In-line Rheometry of Micro Cement Based Grouts - A Promising New Industrial Application of The Ultrasound Based UVP-PD Method. *Applied Rheology*, 22(4), 42783-42794.
- Wiklund, J. a. (2014). Flow-Viz - A fully integrated and commercial in-line fluid characterization system for industrial applications. *Annual transactions of the nordic rheology society*, 22.
- Wiklund, J. a. (2014). In-line rheometry of particulate uspensions by pulsed ultrasound velocimetry combined with presure difference method. *Applied Rheology*, 22(4), 42232-42242.
- Wilkinson, W. (1960). *Non-Newtonian Fluids*. London-Oxford-New York-Paris: Pergamom Press.
- Yu, A. a. (2006). Transit-time broadening in pulsed Doppler ultrasound: a generalized amplitude modulation model. *IEEE Tran Ultrasonnd Ferroelectric Freq Control*, 53(3), 530-541.